# Structure-activity relationship study of CXCR4 antagonists bearing the cyclic pentapeptide scaffold: identification of the new pharmacophore†

**Tomohiro Tanaka,[a] Hiroshi Tsutsumi,*[a] Wataru Nomura,[a] Yasuaki Tanabe,[a] Nami Ohashi,[a] Ai Esaka,[b] Chihiro Ochiai,[a] Jun Sato,[a] Kyoko Itotani,[a] Tsutomu Murakami,[c] Kenji Ohba,[c] Naoki Yamamoto,[c] Nobutaka Fujii[b] and Hirokazu Tamamura*[a]**

*Received 14th July 2008, Accepted 28th August 2008*
*First published as an Advance Article on the web 17th October 2008*
**DOI: 10.1039/b812029c**

A highly potent CXCR4 antagonist **2** [cyclo (-D-Tyr[1]-Arg[2]-Arg[3]-Nal[4]-Gly[5]-)] has previously been identified by screening cyclic pentapeptide libraries that were designed based on pharmacophore residues of a 14-residue peptidic CXCR4 antagonist **1**. In the present study, D-Tyr and Arg in peptide **2** were replaced by a bicyclic aromatic amino acid and a cationic amino acid, respectively, and their binding activity for CXCR4 was evaluated for identification of the novel pharmacophore.

## Introduction

The chemokine receptor CXCR4 is a membrane protein, which belongs to the G-protein coupled receptor family.[1,2] Interaction of CXCR4 with its endogenous ligand stromal-cell derived factor-1α (SDF-1α)/CXCL12 induces various physiological functions: chemotaxis,[3] angiogenesis,[4,5] neurogenesis,[6,7] *etc.* in embryonic stage. On the other hand, CXCR4 is also relevant to multiple diseases: AIDS,[8,9] cancer metastasis,[10] progress of leukemia,[11] rheumatoid arthritis,[12] *etc.* in adulthood. Actually, CXCR4 has been reported to be a potential drug target against these diseases. Thus, CXCR4 antagonists are useful for development of potent therapeutic agents against these diseases.[13–15] To date, various CXCR4 antagonists such as AMD3100[16,17] and KRH-1636[18] have been reported.

A β-sheet-like 14-residue peptide **1** was previously identified by structure optimization of an 18-residue cyclic peptide polyphemusin isolated from horseshoe crabs (Fig. 1).[19,20] In the downsizing of **1**, a cyclic pentapeptide **2** was developed by screening libraries based on four pharmacophore residues [Arg, Arg, 3-(2-naphthyl)alanine (Nal), D-Tyr] found by alanine scanning of **1**.[21]

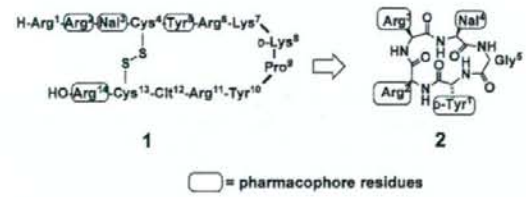


**Fig. 1** Development of a cyclic pentapeptide **2** based the pharmacophore of a CXCR4 antagonistic peptide **1**. Cit = L-citrulline, Nal = L-3-(2-naphthyl)alanine.

We have studied structure-activity-relationships of **2** by various modifications.[22,23] In this paper, design of cyclic pentapeptide library based on the previous structure-activity relationship data led to development of novel analogues of **2** to explore new pharmacophore moieties.

## Biological results and discussion

### Substitution of a large aromatic amino acid for D-Tyr[1] of 2

Our previous data of alanine-scanning of **2** suggested that D-Tyr[1] or Arg[2] was not optimalized.[24] Thus, we attempted to replace these functional groups. According to other previous reports, potent CXCR4 antagonists absolutely contain aromatic and cationic groups.[25] It suggests that these functional groups are involved in binding to CXCR4 mediated by hydrophobic and electrostatic interaction. To evaluate significance of the hydrophobic interaction by aromatic rings, D-Tyr[1] of **2** was replaced by an L/D-bicyclic aromatic amino acid. In addition, four epimers were synthesized to evaluate effects of configuration of amino acids of the 1- and 2- positions (Fig. 2). Compounds **3c** and **3d** with replacement of D-Tyr[1] by D-3-(1-naphthyl)alanine (D-Nal(1)) showed high CXCR4 binding activity ($IC_{50}$ = 0.043 and 0.078 μM, respectively, Table 1), although the potencies were approximately one-third or fifth of that of the parent compound **2** ($IC_{50}$ = 0.015 μM, Table 1). Similarly, compounds **5c** and **5d**, replaced by D-Trp at the 1-position, showed 5–10 fold lower CXCR4 binding activity ($IC_{50}$ = 0.15 and 0.070 μM, respectively, Table 1) than the parent compound **2**. On the other hand, compounds **4c** and **4d** did not show strong CXCR4 binding activity. These data indicates that the spatial position of aromatic ring is essential for the expression of CXCR4 binding activity. In addition, a series of **a** or **b** except for **5a** did not show strong CXCR4 binding activity (all $IC_{50}$ values > 0.3 μM, Table 1). These data indicate that the chirality of L/D-Arg[2] was not important for the expression of CXCR4 binding activity, whereas the chirality of Nal(1)[1] and Trp[1] is influential. The

[a]*Institute of Biomaterials and Bioengineering, Tokyo Medical and Dental University, Chiyoda-ku, Tokyo, 101-0062, Japan. E-mail: tsutsumi.mr@tmd.ac.jp, tamamura.mr@tmd.ac.jp; Fax: 813 5280 8039; Tel: 813 5280 8036*
[b]*Graduate School of Pharmaceutical Sciences, Kyoto University, Sakyo-ku, Kyoto, 606-8501, Japan*
[c]*AIDS Research Center, National Institute of Infectious Diseases, Shinjuku-ku, Tokyo, 162-8640, Japan*

† Electronic supplementary information (ESI) available: Characterization data (MS) of novel synthetic compounds. See DOI: 10.1039/b812029c


This journal is © The Royal Society of Chemistry 2008

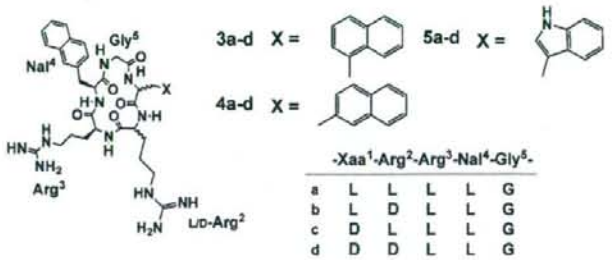


**Fig. 2** Structures of compounds having substitution of an L/D- bicyclic aromatic amino acid for Tyr[1].

**Table 1** Inhibitory activities of the synthetic compounds against binding of [$^{125}$I]-SDF-1α to CXCR4

| Compound no. | $IC_{50}$/μM[a] | Compound no. | $IC_{50}$/μM[a] |
|---|---|---|---|
| **2** | 0.015 | **3c** | 0.043 |
| **3a** | 0.3–2.0 | **4c** | > 2.0 |
| **4a** | 0.3–2.0 | **5c** | 0.15 |
| **5a** | 0.22 | **3d** | 0.078 |
| **3b** | 0.3–2.0 | **4d** | 0.3–2.0 |
| **4b** | 0.3–2.0 | **5d** | 0.070 |
| **5b** | > 2.0 | | |

[a] $IC_{50}$ values are the concentrations for 50% inhibition of the [$^{125}$I]-SDF-1 binding to Jurkat cells. All data are the mean values for at least three experiments.

**Table 2** Inhibitory activities of the synthetic compounds against binding of [$^{125}$I]-SDF-1α to CXCR4

| Compound no. | $IC_{50}$/μM[a] | Compound no. | $IC_{50}$/μM[a] |
|---|---|---|---|
| **2** | 0.015 | **6c** | 0.3–2.0 |
| **6a** | > 2.0 | **7c** | 0.3–2.0 |
| **7a** | 0.3–2.0 | **8c** | > 2.0 |
| **8a** | > 2.0 | **6d** | > 2.0 |
| **6b** | > 2.0 | **7d** | 0.3–2.0 |
| **7b** | 0.045 | **8d** | 0.3–2.0 |
| **8b** | > 2.0 | | |

[a] $IC_{50}$ values are the concentrations for 50% inhibition of the [$^{125}$I]-SDF-1 binding to Jurkat cells. All data are the mean values for at least three experiments.

dependence of CXCR4 binding activity on the chirality at the 1-position might be caused by a conformational change of the peptide backbone.

### Shuffling cationic and aromatic amino acids at the 1- and 2-positions of cyclic pentapeptides

An analogue of **2**, having substitution of Arg[1] and D-4F-phenylalanine[2] for D-Tyr[1] and Arg[2], respectively, was recently found as a strong CXCR4 antagonist.[22] To evaluate effects of the sequential difference of cationic and aromatic groups at the 1- and 2-positions on CXCR4 binding activity, Arg and a large aromatic amino acid (Nal(1), Nal or Trp) were shuffled in the pentapeptide, and four epimers were synthesized in a similar manner (Fig. 3). Synthetic compounds except for **7b** did not show CXCR4 binding activity up to 0.3 μM (Table 2). In particular, a series of **6** and **8** did not show CXCR4 binding activity despite of difference of the chilality of amino acids at the 1- and 2-positions (**6c**, **8d** > 0.3 μM, **6a**, **6b**, **6d**, **8a**, **8b**, **8c** > 2.0 μM). On the other hand, a series of **7**, which introduced L/D-Nal at the 2-position, did not show a serious reduction of CXCR4 binding activity. These data indicated that Nal(1) or Trp might not be appropriate as the amino acid introduced at the 2-position, possibly due to spatial configuration of aromatic rings. **7b** showed the highest CXCR4 binding activity among compounds in this library. Interestingly, **7b** has the opposite chirality and order of the aromatic residue at the 1- and 2-positions compared to the parent compound **2**.

### Evaluation of anti-HIV activity and cytotoxicity

Anti-HIV activity and cytotoxicity of compounds **5c**, **5d** and **7b** that showed moderate CXCR4 binding activity and have a characteristic sequence and conformation were evaluated. Since CXCR4 is a coreceptor for an X4-HIV-1 entry, CXCR4 antagonists have anti-HIV activity.[8,9] Anti-HIV activities of compounds **5d** and **7b** ($EC_{50}$ = 0.19 and 0.26 μM, respectively, Table 3) were nearly equal

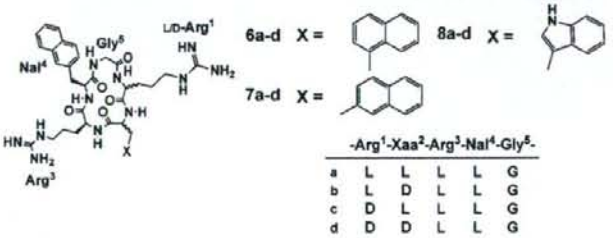


**Fig. 3** Structures of compounds having L/D-Arg[1] and an L/D-bicyclic aromatic amino acid.[2]

Table 3 Anti-HIV activity and cytotoxicity of the synthetic compounds

| Compound no. | $EC_{50}$/μM[a] | $CC_{50}$/μM[b] |
|---|---|---|
| AZT | 0.077 | > 10 |
| 1 | 0.044 | > 10 |
| 2 | 0.15 | > 10 |
| 5c | 0.70 | > 10 |
| 5d | 0.19 | > 10 |
| 7b | 0.26 | > 10 |

[a] $EC_{50}$ values are based on the inhibition of HIV-induced cytopathogenicity in MT-4 cells. [b] $CC_{50}$ values are based on the reduction of the viability of MT-4 cells. All data are the mean values for at least three experiments.

to that of **2** ($EC_{50}$ = 0.15 μM, Table 3). Interestingly, CXCR4 binding activity of **5d** ($IC_{50}$ = 0.070 μM, Table 1) was lower than that of **7b** ($IC_{50}$ = 0.045 μM), whereas anti-HIV activity of **5d** ($EC_{50}$ = 0.19 μM, Table 3) was slightly higher than that of **7b** ($EC_{50}$ = 0.26 μM). In addition, all tested compounds did not show significant cytotoxicity ($CC_{50}$ > 10 μM, Table 3).

## Conclusion

Our first approach screening cyclic pentapeptides, which have substitution of a bicyclic aromatic amino acid at the 1-position, disclosed that D-3-(1-naphthyl)alanine and D-Trp at the 1-position might be alternative pharmacophore moieties, and that introduction of D-amino acid at the 1-position was required to form an optimal cyclic pentapeptide backbone. In addition, compound **5d** showed high anti-HIV activity, comparable to that of compound **2**.

A cyclic pentapeptide library based on shuffling cationic and aromatic amino acids at the 1- and 2-positions of compound **2** was designed. As a result, the order of a cationic amino acid and an aromatic amino acid is significant to maintain strong CXCR4 binding activity of analogues of **2**. Compound **7b**, however, showed the highest CXCR4 binding activity among the present synthetic cyclic pentapeptides. **7b** was proven to be a new type lead, because of the difference of the order of cationic and aromatic residues, and also showed high anti-HIV activity. Finding of compound **7b** indicated that $Arg^1$ and D-$Nal^2$ may be novel pharmacophore moieties in the combination with $Nal^4$ and $Arg^5$. To date, pharmacophore functional groups have been identified to be two guanidino, naphthyl and phenol groups derived from two Arg, Nal and D-Tyr in the cyclic pentapeptide scaffolds. In this study, only guanidino and naphthyl groups have been proven to be indispensable for CXCR4 binding activity. The present data will provide useful approaches for simple designs of new low molecular weight CXCR4 antagonists. These results might also give valuable insights for understanding the ligand-receptor interactions.

## Experimental

### Chemistry

Cyclic peptides were synthesized by Fmoc-based solid-phase synthesis on 2-Chlorotrityl resin followed by cleavage from the resin, cyclization with the diphenylphosphoryl azide and deprotection, as reported previously.[21]

### Cell culture

Human T-cell lines, Jurkat cells and MT-4 cells were grown in RPMI 1640 medium containing 10% heat-inactivated fetal calf serum.

### Virus

An X4 HIV-1 infectious molecular clone pNL4-3 was obtained from the AIDS Research and Reference Reagent Program.[26] The virus NL4-3 was obtained from the culture supernatant of 293T cells transfected with the pNL4-3. Aliquots of the viral stocks were stored at −80 °C until use. The titer of virus stocks was determined by endpoint titration of 5-fold limiting dilutions in MT-4 cells.

### CXCR4 receptor binding assay

Jurkat cells were harvested and centrifugated at 1000 rpm for 5 min. Cells were then resuspended in RPMI buffer (20 mM HEPES, 0.5% bovine serum albumin) and placed in silicone-coated tubes ($5.0 \times 10^5$ cells/120 μL). Cold SDF-1 (final concentration 1 μM, 15 μL/well) and various concentrations of test compounds (10% DMSO, 15 μL/well) were added to the above tubes followed by addition of [$^{125}$I]-SDF-1 (Perkin-Elmer Life Sciences, 0.05 nM, 15 μL/well). After 1 h's incubation on ice, oil (dibutyl phthalate:olive oil = 4:1 (v/v), 500 μL/well) was added followed by centrifugation at 14,000 rpm for 2 min. After removal of aqueous and organic layers and cutting the bottoms from the tubes, the bottoms were placed in RIA-tubes and the CPM was counted by γ-counter. Inhibition percentage of FC131 analogs against the binding of [$^{125}$I]-SDF-1 was calculated by the following equation.[27]

Inhibition (%) = (Et–Ea)/(Et–Ec) × 100

Et: the quantity of radioactivity in the absence of a test compound

Ec: the quantity of radioactivity in the presence of cold SDF-1α as a test compound

Ea: the quantity of radioactivity in the presence of a test compound

### Anti-HIV assay

Anti-HIV-1 activity was determined based on the protection against HIV-1-induced cytopathogenicity in MT-4 cells. Various concentrations of test compounds were added to HIV-1 infected MT-4 cells at multiplicity of infection (MOI) of 0.001 and placed in wells of a flat-bottomed microtiter tray ($2.0 \times 10^4$ cells/well). After 5 days' incubation at 37 °C in a $CO_2$ incubator, the number of viable cells was determined using the 3-(4,5-dimethylthiazol-2-yl)-2,5-diphenyltetrazolium bromide (MTT) method.


## Acknowledgements

This work was supported by Grant-in-Aid for Scientific Research from the Ministry of Education, Culture, Sports, Science, and Technology of Japan, and Health and Labour Sciences Research Grants from Japanese Ministry of Health, Labor, and Welfare.


## References


1 M. Loetscher, T. Geiser, T. O'Reilly, R. Zwahlen, M. Baggiolini and B. Moser, *J. Biol. Chem.*, 1994, **269**, 232–237.




This journal is © The Royal Society of Chemistry 2008

2 B. J. Rollins, *Blood*, 1997, **90**, 909–928.
3 C. C. Bleul, R. C. Fuhlbrigge, J. M. Casanovas, A. Aiuti and T. A. Springer, *J. Exp. Med.*, 1996, **2**, 1101–1109.
4 K. Tachibana, S. Hirota, H. Iizasa, H. Yoshida, K. Kawabata, Y. Kataoka, Y. Kitamura, K. Matsushima, N. Yoshida, S. Nishikawa, T. Kishimoto and T. Nagasawa, *Nature*, 1998, **393**, 591–594.
5 T. Nagasawa, S. Hirota, K. Tachibana, N. Takakura, S. Nishikawa, Y. Kitamura, N. Yoshida, H. Kikutani and T. Kishimoto, *Nature*, 1996, **382**, 635–638.
6 Y. Zhu, Y. Yu, X. C. Zhang, T. Nagasawa, J. Y. Wu and Y. Rao, *Nat. Neurosci.*, 2002, **5**, 719–720.
7 R. K. Stumm, C. Zhou, T. Ara, F. Lazarini, M. Dubois-Dalcq, T. Nagasawa, V. Hollt and S. Schulz, *J. Neurosci.*, 2003, **23**, 5123–5130.
8 E. Oberlin, A. Amara, F. Bachelerie, C. Bessia, J. L. Virelizier, F. Arenzana-Seisdedos, O. Schwartz, J. M. Heard, I. Clark-Lewis, D. L. Legler, M. Loetscher, M. Baggiolini and B. Moser, *Nature*, 1996, **382**, 833–835.
9 Y. Feng, C. C. Broder, P. E. Kennedy and E. A. Berger, *Science*, 1996, **272**, 872–877.
10 A. Müller, B. Homey, H. Soto, N. Ge, D. Catron, M. E. Buchanan, T. Mcclanahan, E. Murphy, W. Yuan, S. M. Wagner, J. L. Barrera, A. Mohar, E. Vera'stegui and A. Zlotnik, *Nature*, 2001, **410**, 50–56.
11 J. A. Burger, M. Burger and T. J. Kipps, *Blood*, 1999, **94**, 3658–3667.
12 T. Nanki, K. Hayashida, H. S. El-Gabalawy, S. Suson, K. Shi, H. J. Girschick, S. Yavuz and P. E. Lipsky, *J Immunol*, 2000, **165**, 6590–6598.
13 T. Murakami, T. Nakajima, Y. Koyanagi, K. Tachibana, N. Fujii, H. Tamamura, N. Toshida, M. Waki, A. Matsumoto, O. Yoshie, T. Kishimoto, N. Yamamoto and T. Nagasawa, *J. Exp. Med.*, 1997, **186**, 1389–1393.
14 H. Tamamura, A. Hori, N. Kanzaki, K. Hiramatsu, M. Mizumoto, H. Nakashima, N. Yamamoto, A. Otaka and N. Fujii, *FEBS Lett.*, 2003, **550**, 79–83.
15 H. Tamamura, M. Fujisawa, K. Hiramatsu, M. Mizumoto, H. Nakashima, N. Yamamoto, A. Otaka and N. Fujii, *FEBS Lett.*, 2004, **569**, 99–104.
16 D. Schols, S. Struyf, J. Van Damme, J. A. Este, G. Henson and E. DeClarcq, *J. Exp. Med.*, 1997, **186**, 1383–1388.
17 G. A. Donzella, D. Schols, S. W. Lin, J. A. Este and K. A. Nagashima, *Nat. Med.*, 1998, **4**, 72–76.
18 K. Ichiya, S. Yokoyama-Kumakura, Y. Tanaka, R. Tanaka, K. Hirose, K. Bannai, T. Edamatsu, M. Yanaka, Y. Niitani, N. Miyano-Kurosaki, H. Takaku, Y. Koyanagi and N. Yamamoto, *Proc. Natl. Acad. Sci. USA*, 2003, **100**, 4185–4190.
19 Tamamura, Y. Xu, T. Hattori, X. Zhang, R. Arakaki, K. Kanbara, A. Omagari, A. Otaka, T. Ibuka, N. Yamamoto, H. Nakashima and N. Fujii, *Biochem. Biophys. Res. Commun.*, 1998, **253**, 877–882.
20 M. Masuda, H. Nakashima, T. Ueda, H. Naba, R. Ikoma, A. Otaka, Y. Terakawa, H. Tamamura, T. Ibuka, T. Murakami, Y. Koyanagi, M. Waki, A. Matsumoto, N. Yamamoto and N. Fujii, *Biochem. Biophys. Res. Commun.*, 1992, **189**, 845–850.
21 N. Fujii, S. Oishi, K. Hiramatsu, T. Araki, S. Ueda, H. Tamamura, A. Otaka, S. Kusano, S. Terakubo, H. Nakashima, J. A. Broach, J. O. Trent, Z. Wang and S. C. Peiper, *Angew. Chem. Int. Ed.*, 2003, **42**, 3251–3253.
22 H. Tamamura, T. Araki, S. Ueda, Z. Wang, S. Oishi, A. Esaka, J. O. Trent, H. Nakashima, N. Yamamoto, S. C. Peiper, A. Otaka and N. Fujii, *J. Med. Chem.*, 2005, **48**, 3280–3289.
23 H. Tamamura, A. Esaka, T. Ogawa, T. Araki, S. Ueda, Z. Wang, J. O. Trent, H. Tsutsumi, H. Masuno, H. Nakashima, N. Yamamoto, S. C. Peiper, A. Otaka and N. Fujii, *Org. Biomol. Chem.*, 2005, **3**, 4392–4394.
24 S. Ueda, S. Oishi, Z. Wang, T. Araki, H. Tamamura, J. Cluzeau, H. Ohno, S. Kusano, H. Nakashima, J. O. Trent, S. C. Peiper and N. Fujii, *J. Med. Chem.*, 2007, **50**, 192–198.
25 W. Zhan, Z. Liang, A. Zhu, S. Kurtkaya, H. Shim, J. P. Snyder and D. C. Liotta, *J.Med. Chem.*, 2007, **50**, 5655–5664.
26 A. Adachi, H. E. Gendelman, S. Koenig, T. Folks, R. Willey, A. Rabson and M. A. Martin, *J Virol.*, 1986, **59**, 284–291.
27 H. Tamamura, K. Hiramatsu, S. Kusano, S. Terakubo, N. Yamamoto, J. O. Trent, Z. Wang, S. C. Peiper, H. Nakashima, A. Otaka and N. Fujii, *Org. Biomol. Chem.*, 2003, **1**, 3656–3662.

NOTE *Virology*

# Inhibitory Effect of Newly Developed CXC-Chemokine Receptor 4 Antagonists on the Infection with Feline Immunodeficiency Virus

Fuminori MIZUKOSHI[1], Kenji BABA[1], Yuko GOTO-KOSHINO[1], Asuka SETOGUCHI-MUKAI[1], Yasuhito FUJINO[1], Koichi OHNO[1], Hirokazu TAMAMURA[2], Shinya OISHI[3], Nobutaka FUJII[3] and Hajime TSUJIMOTO[1]*

[1]*Department of Veterinary Internal Medicine, Graduate School of Agricultural and Life Sciences, The University of Tokyo, 1–1–1 Yayoi, Bunkyo-ku, Tokyo 113–8657,* [2]*Institute of Biomaterials and Bioengineering, Tokyo Medical and Dental University, Chiyoda-ku, Tokyo 101–0062 and* [3]*Graduate School of Pharmaceutical Sciences, Kyoto University, Sakyo-ku, Kyoto 606–8501, Japan*

(Received 16 November 2007/Accepted 29 September 2008)

ABSTRACT. CXC-chemokine receptor 4 (CXCR4) functions as a receptor for feline immunodeficiency virus (FIV). Although we previously found that a CXCR4 antagonist, T140, inhibited the FIV replication *in vitro*, it was not effective in cats infected with FIV because of its low stability in feline serum. To resolve this problem, several T140 derivatives have been developed. Here, we examined the efficacy of T140 analogs, TF14016 and TF14013, on the inhibition of FIV infection. These compounds were shown to significantly inhibit the syncytia formation in CXCR4-expressing cells after co-cultivation with FIV-infected cells and the replication of FIV in a feline lymphoid cultured cell line. These results indicated that TF14016 and TF14013 could be useful as antiviral drugs for cats infected with FIV.

KEY WORDS: CXCR4 antagonist, feline, FIV.

*J. Vet. Med. Sci.* 71(1): 121–124, 2009

CXC-chemokine receptor 4 (CXCR4) is one of the co-receptors for human immunodeficiency virus (HIV) and feline immunodeficiency virus (FIV) and necessary for the cell entry of both viruses [2, 3, 16, 23]. Therefore, blockade of CXCR4 has been expected to be a novel therapeutic strategy in HIV and FIV infections. Previous studies using a natural ligand for CXCR4, stromal cell derived factor-1 (SDF-1), revealed its inhibitory effect against HIV and FIV infections by blocking CXCR4 [4, 5, 8, 10, 16], but indicated its problematic side effect such as marked inflammation after injection *in vivo* [13]. Several CXCR4 antagonists, AMD3100, T22 and T140, were also shown to inhibit HIV infection [6, 7, 17] in cultured cells, but there is no report showing their clinical use because of their instability and strong side effect *in vivo*.

T22 is a derivative of a peptide derived from horseshoe crab blood cells [12]. This peptide consisting of 18-amino acid residues binds specifically to CXCR4 on human cells and inhibits the entry of HIV, however, it does not activate the target cells. Its derivative, T140, is unstable due to the cleavage of C-terminal $Arg^{14}$ in serum and liver homogenate. However, the C-terminally amidated analogs of T140, TF14016 and TF14013, were shown to be bio-stable by virtue of stabilization of the $Arg^{14}$ and possess high antiviral activity, low cytotoxicity, and *in vivo* stability [19]. In this study, we examined the inhibitory effect of TF14016 and TF14013 on the infection with FIV in cultured cells. These compounds were prepared as described previously [19] (Table 1). They were dissolved in water at 1 mM and kept in a freezer at –20°C until use for the assays.

First, we investigated whether TF14016 and TF14013 interact with feline CXCR4. The 3201 cells, which showed strong expression of cell surface CXCR4, were pretreated with 4 $\mu$M of these compounds on ice for 30 min. Then, these cells were reacted with an anti-CXCR4 monoclonal antibody (clone 44717) (R & D systems, Minneapolis, MN) in flow cytometric analysis (FCM) buffer (2% fetal calf serum in PBS) on ice for 30 min. The cells were washed twice with FCM buffer and then incubated with fluorescein isothiocyanate (FITC)-conjugated goat anti-mouse IgG antibody for 30 min on ice. The cells were washed twice with FCM buffer and analyzed with a flow cytometer (FACSCalibur) (Becton Dickinson Immunocytometry systems, San Jose, CA). The fluorescence intensity of 3201 cells detected by clone 44717 was remarkably diminished when the cells were preincubated with both of the compounds (Fig. 1). Clone 44717 was shown to bind to the extracellular loop 2 (E-L2) region of human and feline CXCR4 in the N-terminal domain [1]. The previous report showed that T140 compounds physically bind to E-L2 region of human CXCR4 [22]. Moreover, the E-L2 region was shown to be the most important site in feline CXCR4 for the interaction with FIV envelope protein [23]. Consequently, it is conceivable that the masking of E-L2 region with the T140 analogs results in

Table 1. Amino acid sequence of T140 analogs

| |
|---|
| TF14016<br>4F-benzoly-Arg-Arg-Nal-Cys-Try-Cit-Lys-DLys-Pro-Tyr-Arg-Cit-Cys-Arg-$NH_2$ |
| TF14013<br>4F-benzoly-Arg-Arg-Nal-Cys-Try-Cit-Lys-DGlu-Pro-Tyr-Arg-Cit-Cys-Arg-$NH_2$ |

* CORRESPONDENCE TO: TSUJIMOTO, H., Department of Veterinary Internal Medicine, Graduate School of Agricultural and Life Sciences, The University of Tokyo, 1–1–1 Yayoi, Bunkyo-ku, Tokyo 113–8657, Japan.
e-mail: atsuji@mail.ecc.u-tokyo.ac.jp

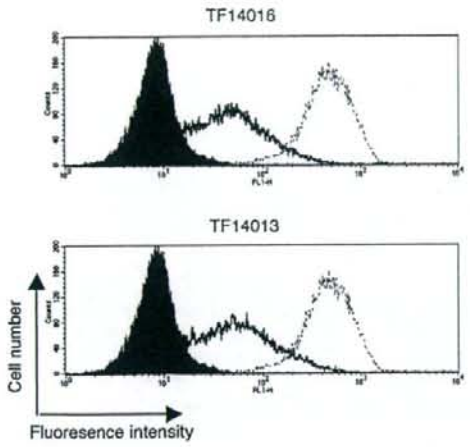


Fig. 1. Fow cytometric analysis to show the inhibitory effect of TF14016 and TF14013 on the binding of anti-CXCR4 monoclonal antibody in 3201 cells. The 3201 cells were treated with the anti-CXCR4 antibody in the presence (thick solid line) or absence (light solid line) of each compound (4 $\mu$M). As a control, the 3201 cells were treated with an isotype control antibody (filled histogram). Then, these cells were treated with FITC-conjugated anti-mouse IgG as a secondary antibody for the flow cytometric analysis.

the interference of the interaction between CXCR4 and FIV envelope protein.

HeLa cells were seeded in Dulbecco's Modified Eagle's Medium (DMEM) and cultured overnight to form monolayers. On the following day, TF14016 or TF14013 (4 $\mu$M each) was added, and the cells were cultured at 37°C for 1 hr. Then, CRFK/FIV cells [15] were added into each of the wells. After 24 hr, the cells were fixed with methanol and stained with Wright and Giemsa solutions. After co-cultivation with CRFK/FIV cells, a number of syncytia were observed as reported by Willet *et al.* [23]. When the HeLa cells were pretreated with either TF14016 or TF14013, the syncytia formation in HeLa cells after co-cultivation with CRFK/FIV cells was remarkably inhibited (Fig. 2). Syncytia formation inhibition rates by the treatment with TF14016 and TF14013 (4 $\mu$M) were 98.1% and 96.2%, respectively, which were calculated as [(number of syncytia in the presence of the compound–number of spontaneously formed syncytia)/(number of syncytia in the absence of the compounds–number of spontaneously formed syncytia) × 100].

Inhibitory effect of the CXCR4 antagonists on the replication of FIV was examined in Kumi-1 cells which were highly permissive to FIV infection [9]. Prior to the experiment, the CXCR4 antagonists were shown to induce no cytotoxic effect on Kumi-1 cells at their concentrations up to 4 $\mu$M. Kumi-1 cells ($2 \times 10^6$ cells/m*l*) were first treated with each of the CXCR4 antagonist compounds, TF14016 and TF14013 (4 $\mu$M), at 37°C for 1 hr, and then inoculated with a subtype A FIV strain, Sendai-1 [11] (final concentration of reverse transcriptase (RT) activity, 50,000 cpm/m*l*).

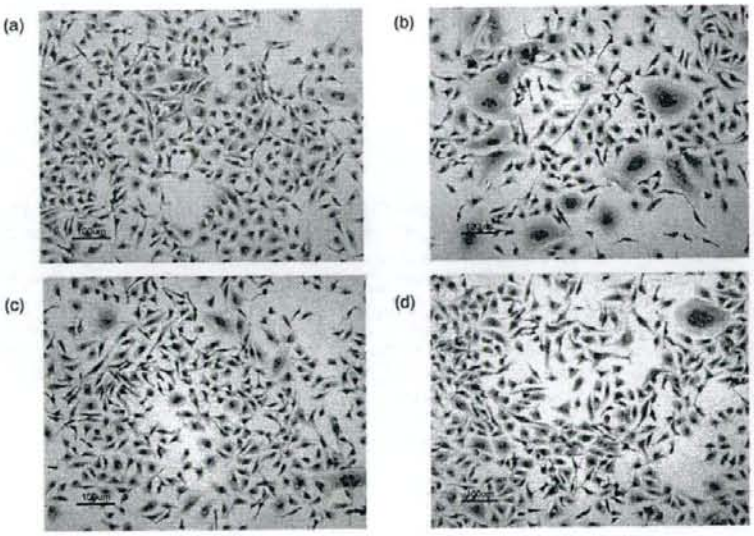


Fig. 2. Inhibition of FIV-mediated syncytia in HeLa cells by the treatment with CXCR4 antagonists. (a) HeLa cells. (b) HeLa cells after cocultivation with CRFK/FIV cells. HeLa cells pretreated with a CXCR4 antagonist, TF14016 (c) or TF14013 (d) (4 $\mu$M), succeedingly co-cultured with CRFK/FIV cells.

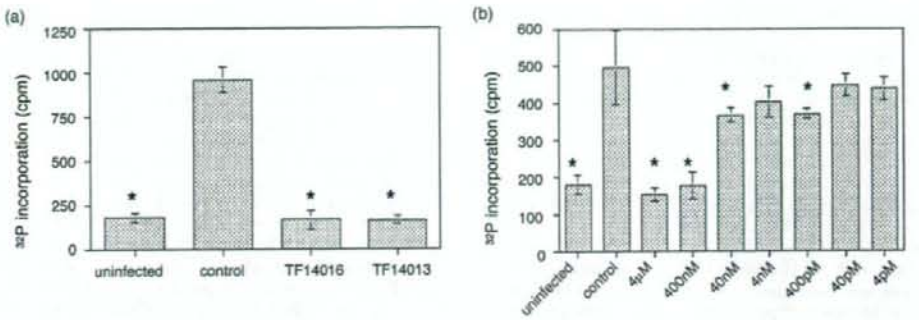


Fig. 3. Inhibitory effect of TF14016 and TF14013 on the replication of FIV in Kumi-1 cells. (a) Untreated Kumi-1 cells (control) and those treated with 4 $\mu$M of TF14016 or TF14013 were inoculated with the FIV Sendai-1 strain. RT activity in the culture supernatants was measured 6 days after inoculation with FIV. RT activity in the culture supernatant of uninfected Kumi-1 cells is also shown (uninfected). (b) Dose-dependency of the antiviral effect of TF14016 on the replication of FIV in Kumi-1 cells. The columns and bars show mean and standard deviations, respectively. Asterisks indicate significant difference from the RT value in the untreated Kumi-1 cells inoculated with FIV.

After adsorption at 37°C for 3 hr, the cells were washed twice with PBS and resuspended to a final cell density of 5 $\times$ $10^5$ cells/m*l*. The cells were cultured in RPMI-1640 medium supplemented with 100 U of human recombinant interleukin-2 (Pharma Biotechnologie, Hannover, Germany) per m*l*. They were passaged 3 days later to dilute the cell density to 5 $\times$ $10^5$ cells/m*l* and were added with each of the fresh compounds. The cell-free supernatants were harvested 6 days after inoculation with FIV to measure RT activity as described previously [8]. When the Kumi-1 cells were pretreated with TF14016 (4 $\mu$M) or TF14013 (4 $\mu$M), the replication of FIV in Kumi-1 cells was significantly inhibited as shown by the decrease of RT activity in their culture supernatants (Fig. 3a). The TF14016 was shown to decrease the RT-activity in the supernatants of the FIV-infected Kumi-1 cells in a dose-dependent manner (Fig. 3b).

The C-terminally amidated analogs of T140 as used in this study were shown to have a potential efficacy against HIV infection [19] as well as rheumatoid arthritis and tumor metastasis mouse models [18, 20]. Additionally, previous studies demonstrated that these compounds were considerably stable in feline serum [21] and effectively inhibited feline SDF-1-induced migration of a feline mammary tumor cell line [14]. In this study, these compounds were shown to significantly inhibit FIV replication at the cell entry level. Thus, it is reasonable to suppose that the administration of these new T140 analogs may exert their antiviral effect in cats infected with FIV. However, because the inhibitory effect of T140 analogs against FIV infection was observed at concentrations more than 400 nM, clinically achievable blood levels remain as a matter to be investigated. Further study is needed to examine the *in vivo* bioavailability, efficacy, and toxicity of the new T140 analogs before their clinical application in cats infected with FIV.

ACKNOWLEDGEMENT. This study was supported by grants from the Japan Health Science Foundation and the Ministries of Education, Science, Sports and Culture, and Health and Welfare of Japan.

REFERENCES

1. Baribaud, F., Edwards, T. G., Sharron, M., Brelot, A., Heveker, N., Price, K., Mortari, F., Alizon, M., Tsang, M. and Doms, R. W. 2001. Antigenically distinct conformations of CXCR4. *J. Virol.* **75**: 8957–8967.
2. Bendinelli, M., Pistello, M., Lombardi, S., Poli, A., Garzelli, C., Matteucci, D., Ceccherini-Nelli, L., Malvaldi, G. and Tozzini, F. 1995. Feline immunodeficiency virus: an interesting model for AIDS studies and an important cat pathogen. *Clin. Microbiol. Rev.* **8**: 87–112.
3. Berger, E. A., Murphy, P. M. and Farber, J. M. 1999. Chemokine receptors as HIV-1 coreceptors: roles in viral entry, tropism, and disease. *Annu. Rev. Immunol.* **17**: 657–700.
4. Bleul, C. C., Farzan, M., Choe, H., Parolin, C., Clark-Lewis, I., Sodroski, J. and Springer, T. A. 1996. The lymphocyte chemoattractant SDF-1 is a ligand for LESTR/fusin and blocks HIV-1 entry. *Nature* **382**: 829–833.
5. De Clercq, E. 2000. Inhibition of HIV infection by bicyclams, highly potent and specific CXCR4 antagonists. *Mol. Pharmacol.* **57**: 833–839.
6. Donzella, G. A., Schols, D., Lin, S. W., Este, J. A., Nagashima, K. A., Maddon, P. J., Allaway, G. P., Sakmar, T. P., Henson, G., De Clercq, E. and Moore, J. P. 1998. AMD3100, a small molecule inhibitor of HIV-1 entry via the CXCR4 co-receptor. *Nat. Med.* **4**: 72–77.
7. Doranz, B. J., Grovit–Ferbas, K., Sharron, M. P., Mao, S. H., Goetz, M. B., Daar, E. S., Doms, R. W. and O'Brien, W. A. 1997. A small-molecule inhibitor directed against the chemokine receptor CXCR4 prevents its use as an HIV-1 coreceptor. *J. Exp. Med.* **186**: 1395–1400.
8. Endo, Y., Goto, Y., Nishimura, Y., Mizuno, T., Watari, T., Hasegawa, A., Hohdatsu, T., Koyama, H. and Tsujimoto, H. 2000. Inhibitory effect of stromal cell derived factor-1 on the replication of divergent strains of feline immunodeficiency

virus in a feline T-lymphoid cell line. *Vet. Immunol. Immunopathol.* **74**: 303–314.

9. Hohdatsu, T., Hirabayashi, H., Motokawa, K. and Koyama, H. 1996. Comparative study of the cell tropism of feline immunodeficiency virus isolates of subtypes A, B and D classified on the basis of the env gene V3-V5 sequence. *J. Gen. Virol.* 77: 93–100.
10. Hosie, M. J., Broere, N., Hesselgesser, J., Turner, J. D., Hoxie, J. A., Neil, J. C. and Willett, B. J. 1998. Modulation of feline immunodeficiency virus infection by stromal cell-derived factor. *J. Virol.* **72**: 2097–2104.
11. Kakinuma, S., Motokawa, K., Hohdatsu, T., Yamamoto, J. K., Koyama, H. and Hashimoto, H. 1995. Nucleotide sequence of feline immunodeficiency virus: classification of Japanese isolates into two subtypes which are distinct from non-Japanese subtypes. *J. Virol.* **69**: 3639–3646.
12. Nakashima, H., Masuda, M., Murakami, T., Koyanagi, Y., Matsumoto, A., Fujii, N. and Yamamoto, N. 1992. Anti-human immunodeficiency virus activity of a novel synthetic peptide, T22 ([Tyr-5,12, Lys-7]polyphemusin II): a possible inhibitor of virus-cell fusion. *Antimicrob. Agents Chemother.* **36**: 1249–1255.
13. Nanki, T., Hayashida, K., El-Gabalawy, H. S., Suson, S., Shi, K., Girschick, H. J., Yavuz, S. and Lipsky, P. E. 2000. Stromal cell-derived factor-1-CXC chemokine receptor 4 interactions play a central role in CD4+ T cell accumulation in rheumatoid arthritis synovium. *J. Immunol.* **165**: 6590–6598.
14. Oonuma, T., Morimatsu, M., Nakagawa, T., Uyama, R., Sasaki, N., Nakaichi, M., Tamamura, H., Fujii, N., Hashimoto, S., Yamamura, H. and Syuto, B. 2003. Role of CXCR4 and SDF-1 in mammary tumor metastasis in the cat. *J. Vet. Med. Sci.* **65**: 1069–1073.
15. Osborne, R., Rigby, M., Siebelink, K., Neil, J. C. and Jarrett. O. 1994. Virus neutralization reveals antigenic variation among feline immunodeficiency virus isolates. *J. Gen. Virol.* **75**: 3641–3645.
16. Richardson, J., Pancino, G., Merat, R., Leste-Lasserre, T., Moraillon, A., Schneider-Mergener, J., Alizon, M., Sonigo, P. and Heveker, N. 1999. Shared usage of the chemokine receptor CXCR4 by primary and laboratory-adapted strains of feline immunodeficiency virus. *J. Virol.* **73**: 3661–3671.
17. Schols, D., Este, J. A., Henson, G. and De Clercq, E. 1997. Bicyclams, a class of potent anti-HIV agents, are targeted at the HIV coreceptor fusin/CXCR-4. *Antiviral Res.* **35**: 147–156.
18. Tamamura, H., Fujisawa, M., Hiramatsu, K., Mizumoto, M., Nakashima, H., Yamamoto, N., Otaka, A. and Fujii, N. 2004. Identification of a CXCR4 antagonist, a T140 analog, as an anti-rheumatoid arthritis agent. *FEBS Lett.* **569**: 99–104.
19. Tamamura, H., Hiramatsu, K., Mizumoto, M., Ueda, S., Kusano, S., Terakubo, S., Akamatsu, M., Yamamoto, N., Trent, J. O., Wang, Z., Peiper, S. C., Nakashima, H., Otaka, A. and Fujii, N. 2003. Enhancement of the T140-based pharmacophores leads to the development of more potent and bio-stable CXCR4 antagonists. *Org. Biomol. Chem.* **1**: 3663–3669.
20. Tamamura, H., Hori, A., Kanzaki, N., Hiramatsu, K., Mizumoto, M., Nakashima, H., Yamamoto, N., Otaka, A. and Fujii, N. 2003. T140 analogs as CXCR4 antagonists identified as anti-metastatic agents in the treatment of breast cancer. *FEBS Lett.* **550**: 79–83.
21. Tamamura, H., Omagari, A., Hiramatsu, K., Gotoh, K., Kanamoto, T., Xu, Y., Kodama, E., Matsuoka, M., Hattori, T., Yamamoto, N., Nakashima, H., Otaka, A. and Fujii, N. 2001. Development of specific CXCR4 inhibitors possessing high selectivity indexes as well as complete stability in serum based on an anti-HIV peptide T140. *Bioorg. Med. Chem. Lett.* **11**: 1897–1902.
22. Trent, J. O., Wang, Z. X., Murray, J. L., Shao, W., Tamamura, H., Fujii, N. and Peiper, S. C. 2003. Lipid bilayer simulations of CXCR4 with inverse agonists and weak partial agonists. *J. Biol. Chem.* **278**: 47136–47144.
23. Willett, B. J., Picard, L., Hosie, M. J., Turner, J. D., Adema, K. and Clapham, P. R. 1997. Shared usage of the chemokine receptor CXCR4 by the feline and human immunodeficiency viruses. *J. Virol.* **71**: 6407–6415.

Journal of General Virology (2008), 89, 554–566 DOI 10.1099/vir.0.83186-0

# Impact of glycosylation on antigenicity of simian immunodeficiency virus SIV239: induction of rapid V1/V2-specific non-neutralizing antibody and delayed neutralizing antibody following infection with an attenuated deglycosylated mutant

Chie Sugimoto,[1,2,3] Emi E. Nakayama,[4] Tatsuo Shioda,[4] Francois Villinger,[5] Aftab A. Ansari,[5] Naoki Yamamoto,[1] Yasuo Suzuki,[3,6] Yoshiyuki Nagai[7] and Kazuyasu Mori[1,2,3]

Correspondence
Kazuyasu Mori
mori@nih.go.jp

[1]AIDS Research Center, National Institute of Infectious Diseases, Shinjuku-ku, Tokyo 162-8640, Japan

[2]Tsukuba Primate Research Center, National Institute of Biomedical Innovation, Tsukuba, Ibaraki 305-0843, Japan

[3]CREST, Japan Science and Technology Agency, Kawaguchi, Saitama 332-0012, Japan

[4]Department of Viral Infections, Research Institute for Microbial Diseases, Osaka University, Suita, Osaka 565-0871, Japan

[5]Department of Pathology and Laboratory Medicine, Emory University, Atlanta, GA 30322, USA

[6]Department of Biomedical Sciences, College of Life and Health Sciences, Chubu University, Kasugai, Aichi 487-8501, Japan

[7]Center of Research Network for Infectious Diseases, Riken, Chiyoda-ku, Tokyo 100-0006, Japan

Infection of rhesus macaques with a deglycosylation mutant, Δ5G, derived from SIV239, a pathogenic clone of simian immunodeficiency virus (SIV), led to robust acute-phase viral replication followed by a chronic phase with undetectable viral load. This study examined whether humoral responses in Δ5G-infected animals played any role in the control of infection. Neutralizing antibodies (nAbs) were elicited more efficiently in Δ5G-infected animals than in SIV239-infected animals. However, functional nAb measured by 90% neutralization was prominent in only two of the five Δ5G-infected animals, and only at 8 weeks post-infection (p.i.), when viral loads were already below $10^4$ copies $ml^{-1}$. These results suggest a minimal role for nAbs in the control of the primary infection. In contrast, whilst Ab responses to epitopes localized to the variable loops V1/V2 were detected in all Δ5G-infected animals at 3 weeks p.i., this response was associated with a concomitant reduction in Ab responses to epitopes in gp41 compared with those in SIV239-infected animals. These results suggest that the altered surface glycosylation and/or conformation of viral spikes induce a humoral response against SIV that is distinct from the response induced by SIV239. More interestingly, whereas V1/V2-specific Abs were induced in all animals, these Abs were associated with vigorous Δ5G-specific virion capture ability in only two Δ5G-infected animals that exhibited a functional nAb response. Thus, whereas the deglycosylation mutant infection elicited early virion capture and subsequent nAbs, the responses differed among animals, suggesting the existence of host factors that may influence the functional humoral responses against human immunodeficiency virus/SIV.

Received 25 May 2007
Accepted 7 October 2007

## INTRODUCTION

The precise role of antibody (Ab) responses in the containment of human immunodeficiency virus (HIV) remains a subject of intense study and debate. Besides the classical direct virus neutralization properties, antibodies are also capable of blocking infection via other pathways such as antibody-dependent complement-mediated inactivation of virus (Aasa-Chapman *et al.*, 2005) and antibody-dependent cellular lysis (Ahmad & Menezes, 1996; Forthal *et al.*, 2001). Acquiring an understanding of these various mechanisms for their exploitation in the


0008-3186 © 2008 SGM Printed in Great Britain

development of candidate vaccines has been a major challenge.

The envelope protein (Env) of HIV/simian immunodeficiency virus (SIV) comprises an exterior protein (gp120) and a transmembrane (TM) protein (gp41), and trimers of the gp120/gp41 complexes form viral spikes that promote binding to receptors and co-receptors on the cell membrane for entry into the target cells (Wyatt & Sodroski, 1998). The major viral receptors of HIV/SIV include CD4 and a variety of co-receptors such as CCR5 or CXCR4. One desirable target epitope for neutralizing antibody (nAb) that shows relative conservation across clades is the binding site for the co-receptor (Burton *et al.*, 2004; Zolla-Pazner, 2004); however, this site is conformationally cryptic within the viral spike up until immediately after binding of the viral spike to CD4, providing an effective shielding mechanism to the virus. Another distinct feature of HIV/SIV Env is the extensive glycosylation that also effectively prevents access to antibodies directed at the epitopes (Chen *et al.*, 2005; Wyatt & Sodroski, 1998; Wyatt *et al.*, 1998). The gp120 protein possesses 18–33 Asn–X–Ser/Thr sequences, signals for the attachment of *N*-linked carbohydrate side chains (Leonard *et al.*, 1990; Ohgimoto *et al.*, 1998; Regier & Desrosiers, 1990; Zhang *et al.*, 2004). As the carbohydrate moiety is generally weakly immunogenic and is recognized to a large extent as self by the host immune system, the massive glycans on the surface of viral spikes constitute an immunologically silent facade (Wyatt & Sodroski, 1998; Wyatt *et al.*, 1998). As a result, mature viral spikes are protected from nAb and other host immune responses by a massive carbohydrate 'glycan shield' (Chen *et al.*, 2005; Wyatt & Sodroski, 1998; Wyatt *et al.*, 1998). In fact, a prominent role of carbohydrates of HIV/SIV in evasion from immune surveillance has been reported previously as follows. Variants of SIV that have evolved to acquire additional glycans in the variable regions of Env have increased neutralization resistance compared with the parental virus (Chackerian *et al.*, 1997; Cheng-Mayer *et al.*, 1999). Similarly, the appearance of neutralization escape mutants has been associated with altered glycosylation in HIV-1 evolved during the course of infection (Wei *et al.*, 2003). Conversely, infection with SIV239 mutants with deglycosylated Env (lacking *N*-linked glycosylation sites) in the variable loops V1/V2 of gp120 elicited markedly increased titres of nAb (Reitter *et al.*, 1998). We have reported that a deglycosylation mutant, Δ5G, lacking *N*-linked glycosylation sites at aa 79, 146, 171, 460 and 479 in gp120 of SIV239 displayed an attenuated phenotype when used to infect rhesus macaques (Mori *et al.*, 2001; Ohgimoto *et al.*, 1998). In addition, animals infected with Δ5G exhibited almost sterile protection against rechallenge with SIV239 (Mori *et al.*, 2001).

Thus, we suggest that studies aimed at identifying the mechanisms underlying the early and potent immune control of deglycosylated SIV may provide knowledge for the formulation of effective HIV/SIV vaccines. Studies performed herein were therefore directed at attempts to define more precisely the early humoral responses (both virus-specific nAb and non-nAb) generated after infection with Δ5G in rhesus macaques and to compare these responses with those observed in macaques inoculated with wild-type SIV239, with the rationale that results from such studies may help to identify their potential contribution towards viral control of primary infection.

## METHODS

**Viruses.** The molecular pathogenic clone of SIV239 (Regier & Desrosiers, 1990) and its derived deglycosylated mutant, Δ5G, were used in this study. Δ5G was derived by mutagenesis of an SIV239 infectious DNA clone so that the asparagine residues for *N*-glycosylation at aa 79, 146, 171, 460 and 479 in gp120 were converted to glutamine residues (Fig. 1a) (Ohgimoto *et al.*, 1998). Viral stocks of SIV239 and Δ5G were prepared as reported previously (Mori *et al.*, 2001).

**Peptides.** A series of 72 consecutive 25 mer peptides overlapping by 13 aa were synthesized based on the entire SIV239 Env sequence (Env-1–72). These peptides were synthesized by the Microchemical Facility, Emory University School of Medicine, Atlanta, USA. Another set of 15 mer peptides overlapping by 11 aa around the V1/V2 region in gp120 (V1V2-1–12) was synthesized by Sigma-Aldrich Japan based on the Δ5G sequence (see Fig. 5b). All peptides were dissolved in DMSO diluted in PBS.

**Animal infection.** Juvenile rhesus macaques originating from Myanmar (Burma) (Mm12, Mm13, Mm20, Mm23 and Mm26) or from Laos (Mm07, Mm22 and Mm25) were used following the results of screening for SIV, simian T-cell lymphotropic virus, B virus and type D retrovirus infection, which were all negative prior to inception of the study. All animals were housed in individual cages and maintained according to the rules and guidelines for experimental animal welfare as outlined by the National Institute of Infectious Diseases and National Institute of Biomedical Innovation. Animals were infected intravenously with Δ5G or SIV239 as described previously (Mori *et al.*, 2001).

**Plasma viral load measurements.** SIV infection was monitored by measuring the plasma viral RNA load using a highly sensitive quantitative real-time RT-PCR. Viral RNA was isolated from plasma samples from infected animals using a commercial viral RNA isolation kit (Roche Diagnostics). SIV *gag* RNA was amplified and quantified using a method originally developed by Hofmann-Lehmann *et al.* (2000) using a TaqMan EZ RT-PCR kit (Applied Biosystems). The detection sensitivity of plasma viral RNA by this method was 100 viral RNA copies per ml plasma (given as copies $ml^{-1}$).

**Neutralization assay.** SIV neutralization was tested according to a protocol using CEMx174/SIVLTR-SEAP cells, originally described by Means *et al.* (1997). To measure low levels of nAb, IgG was purified from plasma as described below and concentrated virus stocks were used.

**Anti-gp120 Ab ELISA and anti-Env peptide ELISA.** Recombinant SIV239 gp120 and Δ5G gp120 were expressed utilizing a Sendai virus vector as described previously (Mori *et al.*, 2005; Yu *et al.*, 1997). Culture supernatant containing approximately 2 μg secreted SIV gp120 $ml^{-1}$ was diluted with an equal amount of PBS, dispensed into each well of an ELISA plate and allowed to incubate at 4 °C overnight.

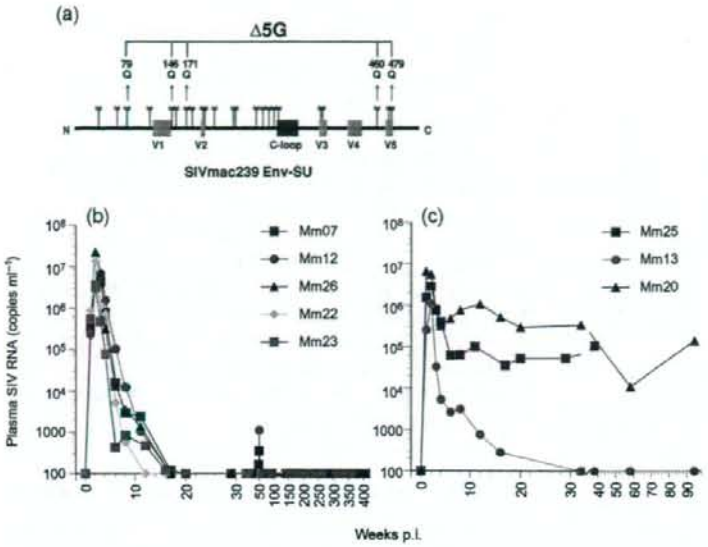


**Fig. 1.** Plasma SIV RNA loads in animals infected with Δ5G or SIV239. (a) *N*-Glycosylation sites in SIV239 gp120 and deglycosylation sites in Δ5G gp120. The locations of 23 *N*-glycosylation sites in SIV239 gp120, variable regions (V1–V5) and cysteine loops (C-loop) are shown. Δ5G was deglycosylated by N→Q substitutions at aa 79, 146, 171, 460 and 479 in Env (Ohgimoto *et al.*, 1998). (b, c) Plasma viral load in Δ5G-infected (b) and SIV239-infected (c) animals was measured in plasma samples using sensitive real-time RT-PCR to indicate when viral loads declined below 100 copies $ml^{-1}$. Three Δ5G-infected animals (Mm07, Mm12 and Mm26) were challenged with SIV239 at 48 weeks p.i.; thus, slightly increased viral loads were detected in those animals during weeks 49–51 p.i. (Mori *et al.*, 2001).

For the peptide ELISA, each peptide was diluted to 0.5 μM with 50 mM carbonate buffer (pH 9.5) and captured on Nunc Immobilizer amino plates (Nalge Nunc) at 4 °C overnight. A 1:100 dilution (150 μl) of the plasma sample to be tested was dispensed into antigen-immobilized plates and incubated at 37 °C for 1 h. Ab responses were detected using peroxidase-conjugated goat anti-monkey IgG and *o*-phenylenediamine. Absorbance was measured at 490 nm.

**Removal of linear V1/V2 epitope-specific Abs from IgG fractions.** A mixture of the peptides (V1V2-9, -10 and -11; see Fig. 5b) was conjugated to a HiTrap NHS-activated HP column (GE Healthcare). IgGs from plasma samples were fractionated using a mAb trap kit (GE Healthcare) and applied to the peptide-conjugated column. The flow-through fractions devoid of anti-V1V2-9, -10 and -11 peptide-specific Abs were collected. The concentration of IgG was determined using a protein assay kit (Bio-Rad).

**Virion capture assay.** The virion capture assay was modified using a method reported by Nyambi *et al.* (1998). ELISA plates were coated with the IgG samples described above at a concentration of 20 μg $ml^{-1}$ in 50 mM carbonate buffer (pH 9.5) and incubated at 4 °C for 48 h. The plates were washed three times with PBS and blocked with 3 % BSA in PBS at 37 °C for 1 h. The plates were then washed three times with serum-free RPMI 1640. Δ5G or SIV239 virion solutions with a $p27^{gag}$ concentration of 15, 7.5 and 3.75 ng in 10 % fetal bovine serum/RPMI 1640 were added to each well of the IgG-coated plate and incubated at 37 °C for 3 h. The wells were washed five times with serum-free RPMI 1640 to remove unbound virus. The virus bound to IgG was lysed using MagNA Pure LC Lysis/Binding Buffer (Roche Diagnostics). The viral lysates were subjected to viral RNA purification using a MagNA Pure Compact nucleic acid purification kit (Roche Diagnostics). The copy number of the isolated SIV RNA was determined by real-time RT-PCR for SIV239 as described above.

**Statistical analysis.** Correlation analysis was done using Spearman's non-parametric rank test and the Mann–Whitney test using GraphPad Prism 4.0 software. Correlations were considered to be statistically significant for values of $P<0.05$.

## RESULTS

### Plasma viral loads of a quintuple deglycosylated SIV239 mutant in rhesus macaques

Eight rhesus macaques were infected intravenously with Δ5G ($n=5$) or SIV239 ($n=3$) (Mori *et al.*, 2001). Plasma viral RNA loads were assayed for up to 400 weeks p.i. and the data obtained in the Δ5G-infected (Fig. 1b) or SIV239-infected (Fig. 1c) animals were plotted. Both Δ5G and SIV239 replicated with similar kinetics during the early phase of primary infection for up to 4 weeks p.i. However, subsequent to this acute infection phase, virus replication was markedly different in the two groups of monkeys: SIV239-infected animals exhibited viral load set points around $10^5$ copies $ml^{-1}$ in two of three animals, with one animal (Mm13) having an undetectable viral load (<100 copies $ml^{-1}$) by 30 weeks p.i. (Fig. 1c). In contrast, the Δ5G-infected animals showed uniformly controlled viraemia reaching undetectable levels by 12–16 weeks p.i. and maintained this control for more than 6 years p.i. (Fig. 1b).

### nAb response in Δ5G-infected animals

Although failure to detect a nAb response is characteristic of SIV239-infected rhesus macaques (Johnson *et al.*, 2003; Means *et al.*, 1997), the rapid control of viraemia in Δ5G-infected animals prompted us to determine whether nAb played a role in this control of viraemia. We hypothesized that the deglycosylation might lead to the elicitation of a markedly more vigorous nAb response than infection with SIV239. To maximize the detection sensitivity of weak nAb responses at early time points p.i., an assay that measures neutralization titres based on 50 % inhibition of virus replication ($IC_{50}$) in $CD4^+$ T-cell lines was initially used.

Consistent with the reported results in SIV239-infected animals, no appreciable nAb titre was detected in two animals (Mm13 and Mm25), despite the fact that viral load in Mm13 was distinctively decreased by 30 weeks p.i. However, we observed a rare animal (Mm20) that elicited a robust nAb response against SIV239 and a relatively delayed nAb response against Δ5G, despite the maintenance of a high viral load (Fig. 2a). These results indicated the lack of correlation of nAb response with viral load in SIV239-infected animals. In contrast, nAb was detected in two Δ5G-infected animals (Mm07 and Mm22) starting at 8 weeks p.i. and in two additional animals (Mm12 and Mm23) at 12 weeks p.i. (Fig. 2b, left panel). These titres peaked at either 12 or 18 weeks p.i., and the peak was followed by a decrease in titre that varied among animals. Mm12 and Mm23, which exhibited nAb induction at 12 weeks p.i., had essentially low titres, whilst Mm07 and Mm22, which exhibited nAb induction at an earlier time point, maintained vigorous nAb titres of $>1:100$. Of note, plasma from Mm26 did not contain detectable levels of nAb at any time p.i. In contrast, nAb against SIV239 was not induced in any of the Δ5G-infected animals (Fig. 2b, right panel). As low-level nAb may play a role in control of virus replication, purified IgG from the plasma samples was used to measure neutralizing activity. However, the results from the purified IgG corresponding to the plasma at a 1:3 dilution did not change the kinetics of nAb response in Δ5G-infected animals (data not shown).

In experiments where the passive administration of monoclonal HIV nAb successfully prevented the infection of macaques with simian–human immunodeficiency virus, the results unequivocally indicated that high titres of nAb were needed to achieve such protection (Nishimura *et al.*, 2002). In consideration of these results, data were recalculated based on a cut-off value of 90 % inhibition of virus replication ($IC_{90}$) in $CD4^+$ T-cell lines. As a result, nAb responses were detected in only two of the animals, Mm07 and Mm22, but with titres of 1:100 and 1:500, respectively (Fig. 2b, middle panel). Next, we examined the correlation between viral load and nAb titre at 8 and 12 weeks p.i. and found that the correlation was not statistically significant (Fig. 2c).

## Anti-gp120 Ab response in Δ5G-infected animals

Next, we measured binding Ab responses against gp120. When the plasma samples were assayed for levels of Ab that bound to SIV239 gp120 or Δ5G gp120, essentially identical values were obtained. Fig. 3 shows the data obtained using SIV239 gp120. Remarkably, anti-gp120 responses during the early period p.i. between the two groups of monkeys were distinct. Whereas anti-gp120-specific Ab responses

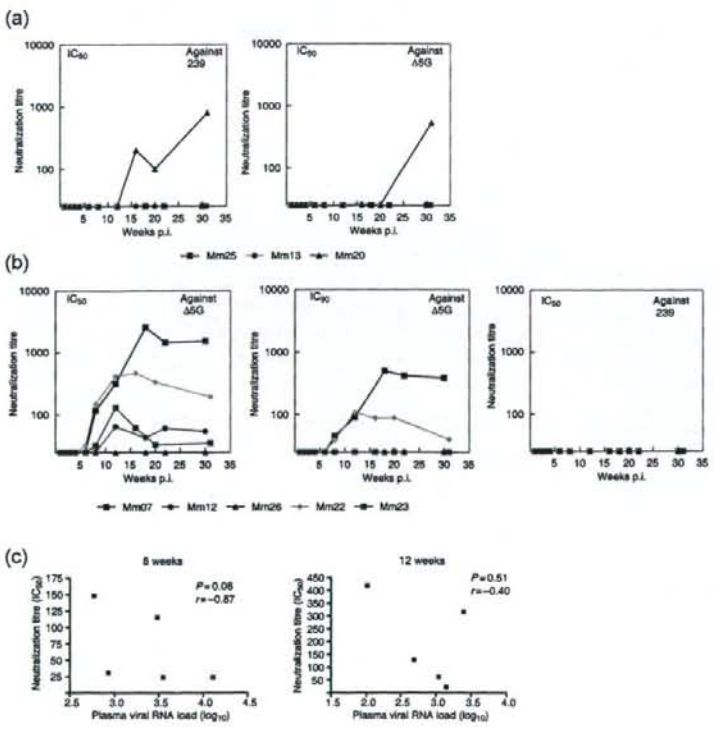


**Fig. 2.** nAb titres in SIV-infected animals. (a) nAb titres in SIV239-infected animals are indicated as the plasma dilution yielding 50 % inhibition ($IC_{50}$) of SIV239 infection (left) or Δ5G infection (right) in CEMx174/SIVLTR-SEAP cells. (b) nAb titres in Δ5G-infected animals are indicated as the plasma dilution that yielded 50 % inhibition ($IC_{50}$, left) and 90 % inhibition ($IC_{90}$, middle) of Δ5G infection or 50 % inhibition of SIV239 infection (right) in CEMx174/SIVLTR-SEAP cells. (c) Correlation between $IC_{50}$ nAb titres and plasma viral RNA load at 8 and 12 weeks p.i. in Δ5G-infected animals.

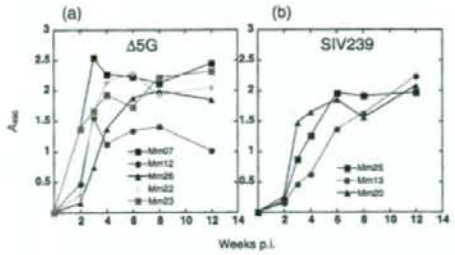


**Fig. 3.** Anti-gp120 Ab responses. Anti-gp120 Ab responses in Δ5G-infected (a) and SIV239-infected (b) animals were indicated as $A_{490}$ using plasma diluted 1 : 100 in an ELISA.

peaked at 3–4 weeks p.i. in Δ5G-infected animals (Fig. 3a), those in SIV239-infected animals remained generally lower and required longer periods of time to reach their peak (Fig. 3b). Of note, whilst anti-gp120 Ab responses did not correlate well with nAb titres in the chronic phase in Δ5G-infected animals, the hierarchy detected in nAb titres (Mm07, Mm22, Mm23, Mm12 and Mm26, in descending order) was similar to that observed for gp120-binding antibodies at 2 weeks p.i. (Fig. 3a).

## Ab responses to linear epitopes in gp120 and gp41 in Δ5G-infected animals differ from those detected in SIV239-infected animals

Next, we examined Ab-binding responses to linear epitopes in plasma samples from infected animals at 8 weeks p.i., as both nAb and anti-gp120-binding Ab were detected at this time point (Figs 2 and 3). We used 72 overlapping peptides encompassing the entire Env sequence of SIV239 for the detection of epitope-specific Ab in plasma samples from Δ5G-infected or SIV239-infected animals. As shown in Fig. 4 and Table 1, the plasma samples reacted with the peptides in six regions: two in gp120 and four in gp41. The regions in gp120 resided in the vicinity of V1/V2, designated region 1 (aa 109–193), and at the C terminus, designated region 2 (aa 493–529). Of note, only linear region 1 was directly affected by selected deglycosylation (aa 146 and 171). The regions in gp41 were located in the ectodomain for region 3 (aa 589–625) and region 4 (aa 660–685), and in the cytoplasmic domain for region 5 (aa 721–757) and region 6 (aa 841–879).

Although Ab responses to most of the peptides recognized in the plasma samples from Δ5G-infected animals were similar to those in SIV239-infected animals, a few peptides were recognized by Abs only in samples from Δ5G-infected animals, and Ab reactivity to some peptides was significantly different between the two groups (Fig. 4b, c and Table 1). Firstly, in region 1, whereas five peptides (Env-10, -12, -13, -14 and -15) were recognized by Abs from Δ5G-infected animals, only three peptides (Env-10, -12 and -13) reacted with Abs from SIV239-infected animals (Fig. 4b and c). Peptide Env-10 was detected by Abs from four Δ5G-infected animals, but from only one of the SIV239-infected animals. Similarly, peptides Env-12 and -13 were detected by Abs from five Δ5G-infected animals and two SIV239-infected animals. In contrast, peptides Env-14 and -15 were detected by Abs from Δ5G-infected animals but not SIV239-infected animals. The specificity of Δ5G infection in the reactivity of peptide Env-14 was statistically significant ($P$=0.0149) (Table 1). Secondly, the reactivity of Ab from Δ5G-infected animals with the peptides in regions 2, 3 and 4 was lower than that recorded with Ab from SIV239-infected animals (Fig. 4b and c). As shown in Table 1, the reduction in Ab reactivity from Δ5G-infected animals to peptide Env-51 (region 3) and peptide Env-56 (region 4) was significant ($P$=0.014 and 0.0053, respectively); however, the reduction in Ab response in region 2 was not significant. In addition, there were no significant differences in the Ab responses to the peptides in regions 5 and 6 between Δ5G-infected and SIV239-infected monkeys (Fig. 4b, c and Table 1).

## A Δ5G-specific linear epitope resides in the region containing the third deglycosylation site (aa 171) between V1 and V2

As region 1 also contained the site of two mutations introduced to limit glycosylation in the Δ5G mutant, we focused additional studies on this region. To identify the Δ5G-specific epitope(s) in region 1, peptide ELISA was performed with 12 newly synthesized shorter peptides based on the Δ5G sequence spanning the V1/V2 region (Fig. 5). Ab reactivity to peptide Env-14 was mapped to peptides V1V2-9–11 (Fig. 5a). Thus, three linear epitopes (encompassed in peptides Env-10, V1V2-3 and V1V2-9–11) were identified within the V1/V2 region (Figs 4 and 5). Whilst two epitopes contained in peptides Env-10 and V1V2-3 were recognized by Ab from both SIV239- and Δ5G-infected animals, the epitope(s) corresponding to peptides V1V2-9–11 was specific to Δ5G infection (Fig. 5a). As the latter contained the third deglycosylation mutation (Figs 1 and 5b, aa 171), Δ5G specificity was probably secondary to the removal of *N*-glycan at this site in SIV239 gp120 (Fig. 5).

## Δ5G-specific Ab responses to linear epitopes in Env elicited immediately following primary infection

In an effort to define the potential relevance of the linear epitope-specific Ab responses in the reduction of acute virus replication in Δ5G-infected animals, we examined the kinetics of Ab reactivity to 12 peptides: Env-10, V1V2-3 and V1V2-9, -10 and -11 for epitopes in region 1; Env-42 and -43 for epitopes in region 2; Env-50 and -51 for epitopes in region 3; Env-56 for epitopes in region 4; and Env-61 and -62 for epitopes in region 5 (Fig. 6). Whilst the induction kinetics of Ab to most peptides were variable in

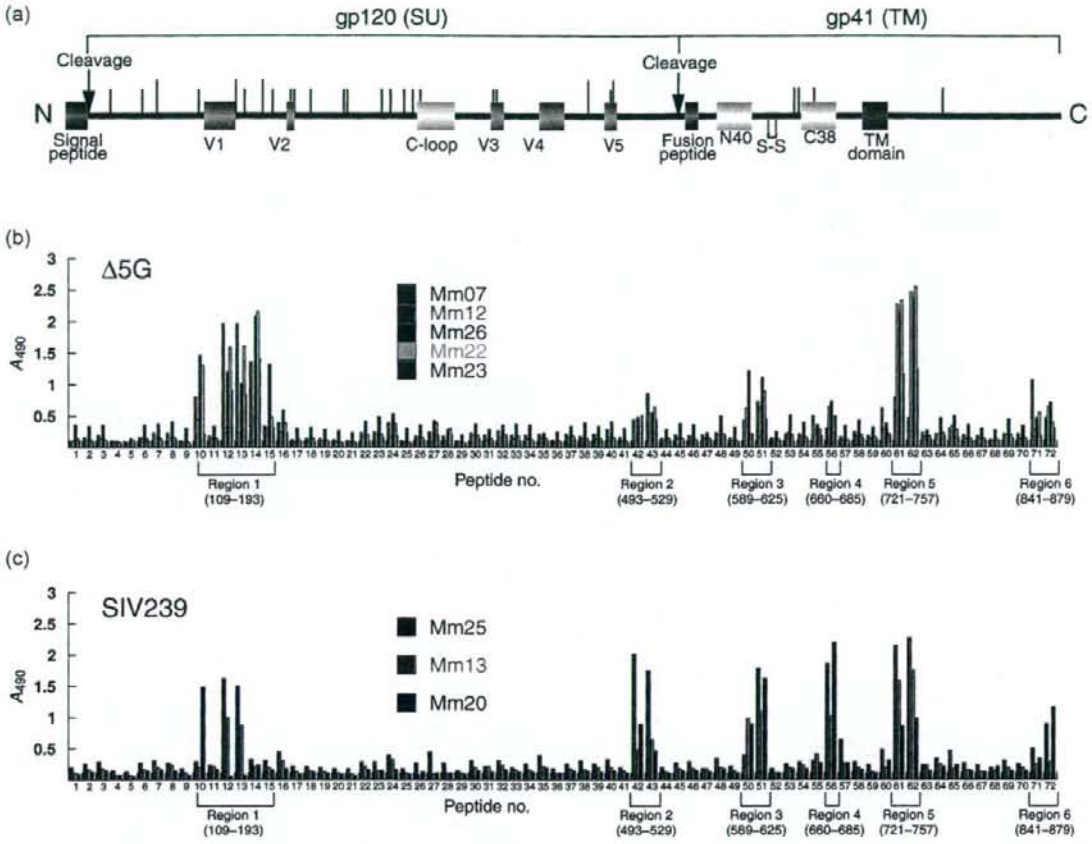


**Fig. 4.** Ab reactivity to synthetic overlapping peptides spanning the entire Env protein. (a) Diagram of SIV239 Env with the locations of the signal peptide (violet box), variable regions (pink boxes), cysteine loop (yellow box), fusion peptide (green box), N-terminal (N40) and C-terminal (C38) heptad repeats (light-blue boxes), membrane-spanning domain (blue box) and *N*-glycosylation sites (vertical bars) (Burns & Desrosiers, 1991; Choi *et al.*, 1994; Liu *et al.*, 2002). Red vertical bars indicate deglycosylation sites (aa 79, 146, 171, 460 and 479) in Δ5G. S-S indicates the indispensable disulfide bond for hairpin loop formation of the TM protein. (b, c) Plasma samples collected from animals infected with Δ5G (b) and SIV239 (c) at 8 weeks p.i. were used to examine Ab reactivity to 72 peptides (25 mers) overlapping by 13 residues each and spanning the entire Env protein. Reactivity was shown by $A_{490}$.

plasma from both groups of animals, Ab to V1V2-9, -10 and -11 was specific for Δ5G-infected animals, with rapid induction following primary infection. Ab responses to Env-61 and -62 were also induced rapidly in animals from the two groups; however, it has already been confirmed by SIV and HIV studies that a linear epitope covered by these peptides is the immunodominant epitope with no association with virus control (Eberle *et al.*, 1997; Kent *et al.*, 1992). In contrast to Ab responses to V1/V2 peptides, whilst Ab to peptides Env-51 and -56 in the gp41 ectodomain were detected in SIV239-infected animals, these reactions were low until at least 12 weeks p.i. in Δ5G-infected animals.

## Properties of Ab against Δ5G-specific linear epitope

Although Ab reactivity to peptide V1V2-9, -10 and -11 was elicited specifically in Δ5G-infected animals, these Abs were non-nAbs, as these binding Abs were detected in all Δ5G-infected animals, including a nAb-undetectable monkey (Mm26), and before nAb was detected. In addition, we attempted to inhibit neutralization by the addition of excess concentrations of V1V2-9, -10 and -11 to the neutralization assay performed with plasma from Δ5G-infected animals collected at 8 and 12 weeks p.i. The reduction of nAb by the addition of an excess amount of

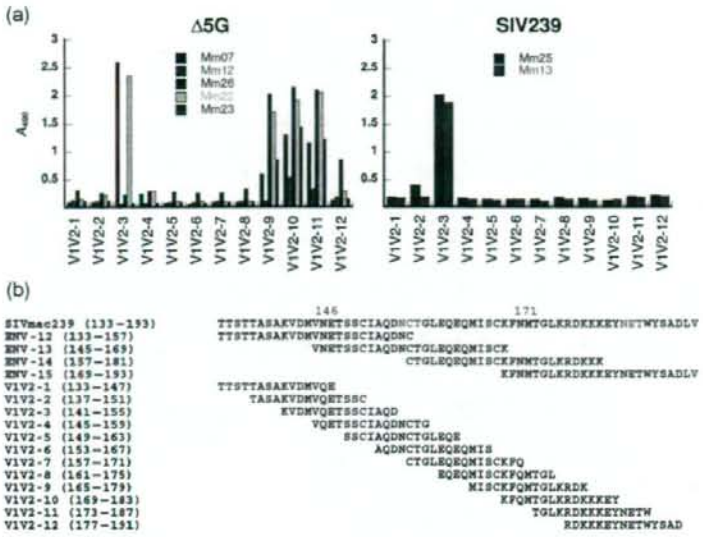


**Fig. 5.** Ab reactivity to linear epitopes in the V1/V2 region of gp120. (a) To define linear epitopes in the V1/V2 region, peptide ELISA was performed using 12 peptides (15 mers) overlapping by 11 residues each. (b) Sequences and positions of the 12 V1/V2 peptides used in (a) and the peptides Env-12 to -15.

peptide was not detected in any samples, confirming that the epitopes targeted by nAb and V1V2-specific Ab were distinct (data not shown).

Next, we tested plasma IgG samples from SIV-infected animals for the quantitative capture of whole virions. IgG fractions of plasma samples from SIV-infected animals collected at 3–4 weeks p.i. were compared for their capacity to capture Δ5G or SIV239 virions. IgG fractions from two Δ5G-infected animals (Mm07 and Mm22) exhibited remarkably higher virion capture activity than those from other animals (Fig. 7a); however, this capture activity was

**Table 1.** Epitope-specific Ab-binding regions in Env and influence of deglycosylation on Ab binding

| Env subunit | Ab-binding region | Peptide no. | Amino acid range | Region | *P* value* |
|---|---|---|---|---|---|
| SU | Region 1 | 10 | 109–133 | V1 | 0.6733 |
| | | 12 | 133–157 | V1 | 0.5678 |
| | | 13 | 145–169 | V1/V2 | 0.5563 |
| | | 14 | 157–181 | V1/V2 | 0.0149† |
| | | 15 | 169–193 | V1/V2 | 0.2385 |
| | Region 2 | 42 | 493–517 | SU C terminus | 0.0822 |
| | | 43 | 505–529 | | 0.3039 |
| TM | Region 3 | 50 | 589–613 | Ectodomain | 0.4791 |
| | | 51 | 601–625 | | 0.0140† |
| | Region 4 | 56 | 660–685 | Ectodomain | 0.0053‡ |
| | Region 5 | 61 | 721–746 | Cytoplasmic domain | 0.6818 |
| | | 62 | 732–757 | | 0.8188 |
| | Region 6 | 71 | 841–865 | Cytoplasmic domain | 0.5237 |
| | | 72 | 853–879 | | 0.2451 |

*A *t*-test was performed by using data in Fig. 4 to determine differences in Ab reactivity between SIV239 infection and Δ5G infection.
†$P<0.05$; ‡$P<0.01$.

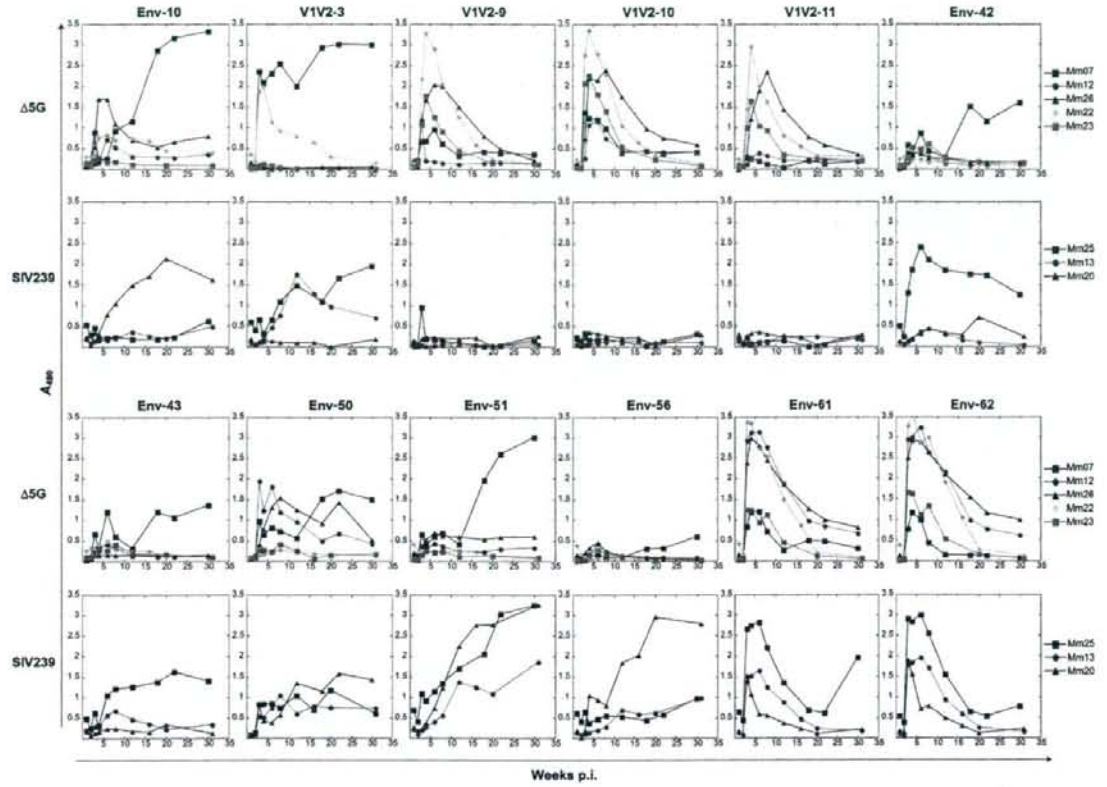


**Fig. 6.** Kinetics of peptide-specific Ab responses in Δ5G-infected and SIV239-infected animals. The kinetics of Ab reaction against peptides selected in the experiments shown in Figs 4 and 5 was determined as $A_{490}$ using plasma diluted 1 : 100 in an ELISA.

Δ5G-specific, as no appreciable capture of SIV239 virion was detected with these samples. Furthermore, this activity was reduced to the level of control IgG (R374) after selective removal of IgG binding to V1V2-9, -10 and -11 peptides, suggesting that virion capture activity is associated with the Δ5G-specific linear epitope Ab (Fig. 7a). By contrast, IgG fractions from SIV239-infected animals collected at 3–4 weeks p.i. did not exhibit appreciable binding activity either to Δ5G virions or SIV239 virions (Fig. 7b). Thus, these results demonstrated that Δ5G infection elicited not only nAb after 8 weeks p.i., but also a much earlier humoral antiviral mechanism in the form of Δ5G-specific virion-binding Ab at 3–4 weeks p.i. in at least two monkeys (Mm07 and Mm22). To examine the relationship between the two antibody activities, we calculated the correlation of virion capture activity of IgG at 3 or 4 weeks p.i. with a peak nAb titre in Δ5G-infected animals (Fig. 2b) and found that this correlation was statistically significant ($r=1$, $P=0.0167$; Fig. 7c).

## DISCUSSION

### nAb response in Δ5G-infected animals

Glycosylation of viral spikes has long been recognized as an effective strategy to evade host (humoral) immune surveillance for several pathogens and for HIV/SIV in particular (Dowling *et al.*, 2007; Fournillier *et al.*, 2001; Haigwood & Stamatatos, 2003; Huso *et al.*, 1988; Reitter *et al.*, 1998). In support of these observations, the data presented here demonstrated that quintuple deglycosylation conferred live attenuated vaccine properties to an SIV239 mutant, Δ5G (Mori *et al.*, 2001); however, a cellular but not humoral response was detected as an immune correlate of the protection of Δ5G-infected animals against SIV239 challenge infection. Therefore, we assumed that the complete control of robust acute virus replication in Δ5G-infected animals beyond the initial cell-mediated control would be due to the development of rapid and effective nAbs. This study indicated that, whereas

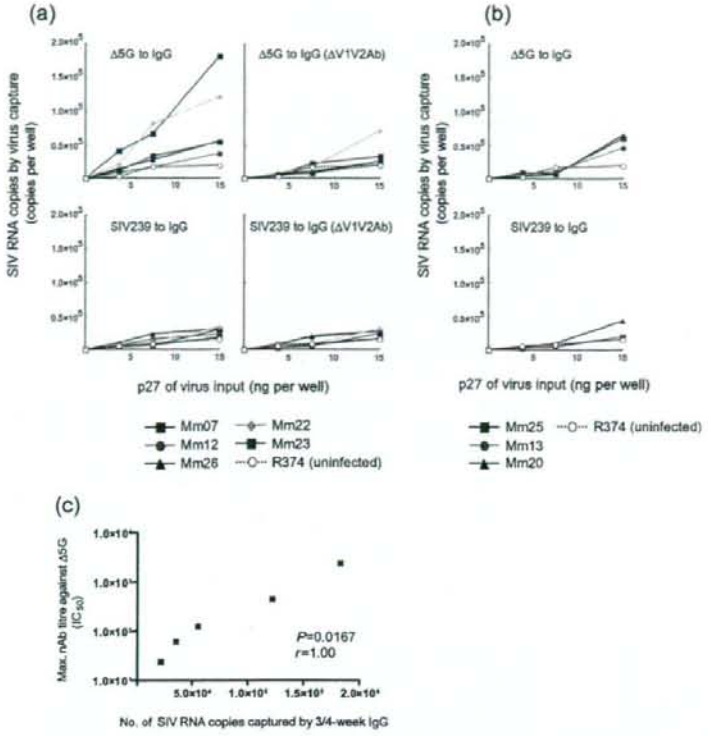


**Fig. 7.** Virion capture activity of IgG from Δ5G-infected and SIV239-infected animals. Virion capture activity of IgG from the plasma of infected animals at 3 or 4 weeks p.i. was determined by increased captured SIV RNA relative to input (3.75, 7.5 and 15 ng $p27^{gag}$) of Δ5G or SIV239. Plasma samples of Δ5G-infected animals (a) and SIV239-infected animals (b) were used for the assay. IgG (ΔV1V2Ab) indicates IgG depleted of Ab binding to V1V2-9, -10 or -11 peptide. R374 was an uninfected monkey. Correlation between virion capture activity at 3 or 4 weeks p.i. and peak nAb titre in Δ5G-infected animals (Fig. 2b) is shown (c).

Δ5G-infected animals clearly exhibited better nAb responses than SIV239-infected animals, the most stringent nAb assay, based on 90 % inhibition, provided evidence of nAb titres in only two of five Δ5G-infected animals and the appearance of these titres trailed the decline of acute viral loads by almost 4 weeks (Figs 1 and 2). Therefore, we concluded that, although deglycosylation did promote better development of nAbs in Δ5G-infection than SIV239 infection, it was still too late to control acute viraemia.

Zinkernagel and co-workers have categorized viruses into two types: 'acutely cytopathic viruses' and 'poorly or non-cytopathic viruses' (Hangartner *et al.*, 2006b). The former contains viruses such as vesicular stomatitis virus in mice and influenza virus in humans, whose control depends primarily on a rapid and potent nAb response. The latter comprises viruses such as lymphocytic choriomenigitis virus in mice, and hepatitis B and C viruses and HIV in humans, against which a nAb response is apparent only following the reduction of primary viraemia, and which establish persistent chronic infections. Accordingly, although the viral loads in Δ5G infection resembled 'acutely cytopathic virus' infections, the kinetics of nAbs still conformed to the 'non-cytopathic virus' category. As the difference in nAb response between the two types of virus is determined by their surface glycoproteins (Pinschewer *et al.*, 2004), this study suggests that the deglycosylation of Δ5G could not change this intrinsic property of SIV239.

## Ab responses to Env peptides in Δ5G-infected animals

Aside from nAb, non-nAb responses to linear epitopes in V1/V2 were specifically induced by 3 weeks p.i. in all Δ5G-infected animals (Figs 4, 5 and 6). The heavy glycosylation of viral spikes clearly prevented access of B-cell receptors to the linear Ab epitopes located within limited regions of gp120 in SIV239, and the reduced glycosylation probably promoted better exposure of these linear epitopes in Δ5G (Fig. 4). Accordingly, the Δ5G-specific epitope in V1/V2 should be closely associated with the deglycosylation mutation at aa 171 in gp120 (Fig. 5). We speculate that this Ab induction might contribute to acute viral suppression in Δ5G infection because of the coincident decrease in peak viraemia (Figs 1 and 6). Non-neutralizing Abs can be divided into those that bind to the intact virion surface and debris-specific Ab. The former non-neutralizing Abs have occasional possibilities for antiviral activities such as antibody-dependent cell-mediated cytotoxicity and complement-mediated virus inactivation (Aasa-Chapman *et al.*, 2005; Ahmad & Menezes, 1996; Forthal *et al.*, 2001; Hangartner *et al.*, 2006a). In fact, readily detectable virion

capture Abs were induced in two of five Δ5G-infected animals (Fig. 7, Mm07 and Mm22). The importance of immediate-early suppression of SIV replication for the long-term containment of infection has been demonstrated by studies of post-exposure anti-retroviral therapy (Lifson *et al.*, 2000; Mori *et al.*, 2000). Thus, the early and complete control of viraemia in Δ5G-infected animals clearly suggests an antiviral mechanism(s) acting as early as 2–4 weeks p.i. Therefore, the early detection of IgG capable of virus capture in Δ5G-infected animals may provide mechanisms capable of contributing to undetectable viral load set points (Fig. 1b). The selective generation of such Ab directed to linear Env epitopes is expected.

Interestingly, deglycosylation in gp120 was also associated with a general reduction in the antigenicity of linear epitopes in gp41: the Ab response against the two epitopes that reside in the regions between the two heptad repeats (aa 601–625) and in the C-terminal heptad repeat (aa 660–685), respectively, was markedly reduced (Fig. 4, Table 1). The former corresponds to the highly conserved immunogenic epitope (Benichou *et al.*, 1993; Gnann *et al.*, 1987; Silvera *et al.*, 1994), and the latter corresponds to an epitope identified in the chronic phase of SIVmac251 infection (Silvera *et al.*, 1994) and corresponds to the nAb epitope of HIV-1 known as 2F5 (Muster *et al.*, 1993), although this linear epitope has not been associated with SIV neutralization (Caffrey *et al.*, 1998). Thus, these epitopes are probably exposed on the surface of viral spikes or their degraded fragments in most SIV and HIV-1 isolates with appropriate glycosylation and correct folding. We believe that the loss of glycosylation might induce a slight conformational change in the gp120 protein backbone, resulting in altered interaction of gp120 and gp41. In fact, the region encompassing the former epitope in gp41 was demonstrated to interact with gp120 (Cao *et al.*, 1993; Maerz *et al.*, 2001; York & Nunberg, 2004). As viral spikes determine virus properties such as viral receptor usage and cell tropism (Kolchinsky *et al.*, 2001; Puffer *et al.*, 2002), different cell populations might be infected in Δ5G-infected animals compared with SIV239 infection. More specifically, because of the distinct properties of the virus, vigorous Δ5G replication in the acute phase did not apparently impair immune function and thus established the control of chronic-phase infection and viral replication.

### Host factors required for functional Ab responses against SIV infection

This study also demonstrated remarkable differences in humoral response with regard to nAb and virion capture Ab among Δ5G-infected animals. However, gp120-specific-binding Ab and the linear epitope-specific Ab were initially induced similarly in all animals. These findings imply that Abs measured by ELISA assay and Abs exhibiting antiviral activity are elicited by different pathways and that the properties associated with functional Abs depend largely on the host and underscore the importance of its genetic background. Rhesus macaques are present in various geographical locations within the Asian continent and are subdivided into many subspecies morphologically and genetically (Smith & McDonough, 2005). Some of the genetic differences among rhesus monkeys of different geographical origins, and especially those involving major histocompatibility complex (MHC) genotypes, probably influence the corresponding differences in immune responses, especially cellular response (Bontrop *et al.*, 1996; O'Connor *et al.*, 2003; Reimann *et al.*, 2005). Schmitz *et al.* (2005) reported that Mamu-A*01-positive rhesus monkeys elicited a significantly higher cellular response and lower nAb titres than those in Mamu-A*01-negative animals at the time of challenge infection of animals vaccinated with live attenuated SIV. They suggested that both humoral and cellular immune responses contributed to the protection against the challenge infection and that the relative contribution of each of the responses may be genetically determined. We observed a similar relationship between nAb and cellular responses among Δ5G-infected animals: two animals (Mm07 and Mm22) elicited a lower cellular response while the other three animals (Mm12, Mm23 and Mm26) elicited a higher cellular response (data not shown). Notably two animals exhibiting highly functional Ab (Mm07 and Mm22) were the offspring of seed animals imported from Laos, whilst the others (Mm12, Mm23 and Mm26) were of Burmese origin, suggesting the potential association of such different humoral and cellular responses with host genetic factors. In clinical studies, considerable concordance of adaptive cellular and humoral responses and HIV evolution in monozygotic twins, but not in brothers, infected with the same virus has been reported (Draenert *et al.*, 2006). HIV-1-exposed but uninfected status with significantly higher neutralizing IgA was linked to genotypes on chromosome 22 (Kanari *et al.*, 2005). In the mouse Friend leukemia virus model, MHC II alleles were determined as host genetic factors required for effective nAb response (Miyazawa *et al.*, 1992) and the host genetic factor was mapped to chromosome 15, which was associated with the clearance of viraemia by nAb (Hasenkrug *et al.*, 1995; Kanari *et al.*, 2005).

Taken together, we speculate that the functional humoral response is determined by host genetic properties similar to the cellular immune response. Thus, gaining knowledge of the genetic requirements for both humoral and cellular containment of viral infections will clearly be of primary importance for vaccine development and therapeutics against HIV and other infectious agents.

## NOTE ADDED IN PROOF

A discrepancy in the SIV239-infected animals Mm13 and Mm20 was noted between the result shown in Fig. 2 and that in a previous report Mori *et al.*, 2001. The nAb

response against SIV239 in Mm20 was confirmed at multiple time points in the present study.

## ACKNOWLEDGEMENTS

We thank Kayoko Ueda for excellent technical assistance and Marcelo Kuroda for critical reading of the manuscript. This study was conducted through the Cooperative Research Program in the Tsukuba Primate Research Center, National Institute of Biomedical Innovation, Japan. This work was supported by AIDS research grants from the Health Sciences Research Grants, from the Ministry of Health, Labour and Welfare in Japan, and from the Ministry of Education, Culture, Sports, Science and Technology in Japan.

## REFERENCES

**Aasa-Chapman, M. M., Holuigue, S., Aubin, K., Wong, M., Jones, N. A., Cornforth, D., Pellegrino, P., Newton, P., Williams, I. & other authors (2005).** Detection of antibody-dependent complement-mediated inactivation of both autologous and heterologous virus in primary human immunodeficiency virus type 1 infection. *J Virol* **79**, 2823–2830.

**Ahmad, A. & Menezes, J. (1996).** Antibody-dependent cellular cytotoxicity in HIV infections. *FASEB J* **10**, 258–266.

**Benichou, S., Venet, A., Beyer, C., Tiollais, P. & Madaule, P. (1993).** Characterization of B-cell epitopes in the envelope glycoproteins of simian immunodeficiency virus. *Virology* **194**, 870–874.

**Bontrop, R. E., Otting, N., Niphuis, H., Noort, R., Teeuwsen, V. & Heeney, J. L. (1996).** The role of major histocompatibility complex polymorphisms on SIV infection in rhesus macaques. *Immunol Lett* **51**, 35–38.

**Burns, D. P. & Desrosiers, R. C. (1991).** Selection of genetic variants of simian immunodeficiency virus in persistently infected rhesus monkeys. *J Virol* **65**, 1843–1854.

**Burton, D. R., Desrosiers, R. C., Doms, R. W., Koff, W. C., Kwong, P. D., Moore, J. P., Nabel, G. J., Sodroski, J., Wilson, I. A. & Wyatt, R. T. (2004).** HIV vaccine design and the neutralizing antibody problem. *Nat Immunol* **5**, 233–236.

**Caffrey, M., Cai, M., Kaufman, J., Stahl, S. J., Wingfield, P. T., Covell, D. G., Gronenborn, A. M. & Clore, G. M. (1998).** Three-dimensional solution structure of the 44 kDa ectodomain of SIV gp41. *EMBO J* **17**, 4572–4584.

**Cao, J., Bergeron, L., Helseth, E., Thali, M., Repke, H. & Sodroski, J. (1993).** Effects of amino acid changes in the extracellular domain of the human immunodeficiency virus type 1 gp41 envelope glycoprotein. *J Virol* **67**, 2747–2755.

**Chackerian, B., Rudensey, L. M. & Overbaugh, J. (1997).** Specific *N*-linked and O-linked glycosylation modifications in the envelope V1 domain of simian immunodeficiency virus variants that evolve in the host alter recognition by neutralizing antibodies. *J Virol* **71**, 7719–7727.

**Chen, B., Vogan, E. M., Gong, H., Skehel, J. J., Wiley, D. C. & Harrison, S. C. (2005).** Structure of an unliganded simian immunodeficiency virus gp120 core. *Nature* **433**, 834–841.

**Cheng-Mayer, C., Brown, A., Harouse, J., Luciw, P. A. & Mayer, A. J. (1999).** Selection for neutralization resistance of the simian/human immunodeficiency virus $SHIV_{SF33A}$ variant in vivo by virtue of sequence changes in the extracellular envelope glycoprotein that modify *N*-linked glycosylation. *J Virol* **73**, 5294–5300.

**Choi, W. S., Collignon, C., Thiriart, C., Burns, D. P., Stott, E. J., Kent, K. A. & Desrosiers, R. C. (1994).** Effects of natural sequence variation on recognition by monoclonal antibodies neutralize simian immunodeficiency virus infectivity. *J Virol* **68**, 5395–5402.

**Dowling, W., Thompson, E., Badger, C., Mellquist, J. L., Garrison, A. R., Smith, J. M., Paragas, J., Hogan, R. J. & Schmaljohn, C. (2007).** Influences of glycosylation on antigenicity, immunogenicity, and protective efficacy of Ebola virus GP DNA vaccines. *J Virol* **81**, 1821–1837.

**Draenert, R., Allen, T. M., Liu, Y., Wrin, T., Chappey, C., Verrill, C. L., Sirera, G., Eldridge, R. L., Lahaie, M. P. & other authors (2006).** Constraints on HIV-1 evolution and immunodominance revealed in monozygotic adult twins infected with the same virus. *J Exp Med* **203**, 529–539.

**Eberle, J., Loussert-Ajaka, I., Brust, S., Zekeng, L., Hauser, P. H., Kaptue, L., Knapp, S., Damond, F., Saragosti, S. & other authors (1997).** Diversity of the immunodominant epitope of gp41 of HIV-1 subtype O and its validity for antibody detection. *J Virol Methods* **67**, 85–91.

**Forthal, D. N., Landucci, G. & Keenan, B. (2001).** Relationship between antibody-dependent cellular cytotoxicity, plasma HIV type 1 RNA, and $CD4^+$ lymphocyte count. *AIDS Res Hum Retroviruses* **17**, 553–561.

**Fournillier, A., Wychowski, C., Boucreux, D., Baumert, T. F., Meunier, J. C., Jacobs, D., Muguet, S., Depla, E. & Inchauspe, G. (2001).** Induction of hepatitis C virus E1 envelope protein-specific immune response can be enhanced by mutation of *N*-glycosylation sites. *J Virol* **75**, 12088–12097.

**Gnann, J. W., Jr, Nelson, J. A. & Oldstone, M. B. (1987).** Fine mapping of an immunodominant domain in the transmembrane glycoprotein of human immunodeficiency virus. *J Virol* **61**, 2639–2641.

**Haigwood, N. L. & Stamatatos, L. (2003).** Role of neutralizing antibodies in HIV infection. *AIDS* **17** (Suppl. 4), S67–S71.

**Hangartner, L., Zellweger, R. M., Giobbi, M., Weber, J., Eschli, B., McCoy, K. D., Harris, N., Recher, M., Zinkernagel, R. M. & Hengartner, H. (2006a).** Nonneutralizing antibodies binding to the surface glycoprotein of lymphocytic choriomeningitis virus reduce early virus spread. *J Exp Med* **203**, 2033–2042.

**Hangartner, L., Zinkernagel, R. M. & Hengartner, H. (2006b).** Antiviral antibody responses: the two extremes of a wide spectrum. *Nat Rev Immunol* **6**, 231–243.

**Hasenkrug, K. J., Valenzuela, A., Letts, V. A., Nishio, J., Chesebro, B. & Frankel, W. N. (1995).** Chromosome mapping of *Rfv3*, a host resistance gene to Friend murine retrovirus. *J Virol* **69**, 2617–2620.

**Hofmann-Lehmann, R., Swenerton, R. K., Liska, V., Leutenegger, C. M., Lutz, H., McClure, H. M. & Ruprecht, R. M. (2000).** Sensitive and robust one-tube real-time reverse transcriptase-polymerase chain reaction to quantify SIV RNA load: comparison of one- versus two-enzyme systems. *AIDS Res Hum Retroviruses* **16**, 1247–1257.

**Huso, D. L., Narayan, O. & Hart, G. W. (1988).** Sialic acids on the surface of caprine arthritis-encephalitis virus define the biological properties of the virus. *J Virol* **62**, 1974–1980.

**Johnson, W. E., Sanford, H., Schwall, L., Burton, D. R., Parren, P. W., Robinson, J. E. & Desrosiers, R. C. (2003).** Assorted mutations in the envelope gene of simian immunodeficiency virus lead to loss of neutralization resistance against antibodies representing a broad spectrum of specificities. *J Virol* **77**, 9993–10003.

**Kanari, Y., Clerici, M., Abe, H., Kawabata, H., Trabattoni, D., Caputo, S. L., Mazzotta, F., Fujisawa, H., Niwa, A. & other authors (2005).** Genotypes at chromosome 22q12–13 are associated with HIV-1-exposed but uninfected status in Italians. *AIDS* **19**, 1015–1024.

**Kent, K. A., Rud, E., Corcoran, T., Powell, C., Thiriart, C., Collignon, C. & Stott, E. J. (1992).** Identification of two neutralizing and 8 non-neutralizing epitopes on simian immunodeficiency virus envelope

using monoclonal antibodies. *AIDS Res Hum Retroviruses* **8**, 1147–1151.

**Kolchinsky, P., Kiprilov, E., Bartley, P., Rubinstein, R. & Sodroski, J. (2001).** Loss of a single *N*-linked glycan allows CD4-independent human immunodeficiency virus type 1 infection by altering the position of the gp120 V1/V2 variable loops. *J Virol* **75**, 3435–3443.

**Leonard, C. K., Spellman, M. W., Riddle, L., Harris, R. J., Thomas, J. N. & Gregory, T. J. (1990).** Assignment of intrachain disulfide bonds and characterization of potential glycosylation sites of the type 1 recombinant human immunodeficiency virus envelope glycoprotein (gp120) expressed in Chinese hamster ovary cells. *J Biol Chem* **265**, 10373–10382.

**Lifson, J. D., Rossio, J. L., Arnaout, R., Li, L., Parks, T. L., Schneider, D. K., Kiser, R. F., Coalter, V. J., Walsh, G. & other authors (2000).** Containment of simian immunodeficiency virus infection: cellular immune responses and protection from rechallenge following transient postinoculation antiretroviral treatment. *J Virol* **74**, 2584–2593.

**Liu, J., Wang, S., Hoxie, J. A., LaBranche, C. C. & Lu, M. (2002).** Mutations that destabilize the gp41 core are determinants for stabilizing the simian immunodeficiency virus-CPmac envelope glycoprotein complex. *J Biol Chem* **277**, 12891–12900.

**Maerz, A. L., Drummer, H. E., Wilson, K. A. & Poumbourios, P. (2001).** Functional analysis of the disulfide-bonded loop/chain reversal region of human immunodeficiency virus type 1 gp41 reveals a critical role in gp120-gp41 association. *J Virol* **75**, 6635–6644.

**Means, R. E., Greenough, T. & Desrosiers, R. C. (1997).** Neutralization sensitivity of cell culture-passaged simian immunodeficiency virus. *J Virol* **71**, 7895–7902.

**Miyazawa, M., Nishio, J., Wehrly, K. & Chesebro, B. (1992).** Influence of MHC genes on spontaneous recovery from Friend retrovirus-induced leukemia. *J Immunol* **148**, 644–647.

**Mori, K., Yasutomi, Y., Sawada, S., Villinger, F., Sugama, K., Rosenwith, B., Heeney, J. L., Uberla, K., Yamazaki, S. & other authors (2000).** Suppression of acute viremia by short-term postexposure prophylaxis of simian/human immunodeficiency virus SHIV-RT-infected monkeys with a novel reverse transcriptase inhibitor (GW420867) allows for development of potent antiviral immune responses resulting in efficient containment of infection. *J Virol* **74**, 5747–5753.

**Mori, K., Yasutomi, Y., Ohgimoto, S., Nakasone, T., Takamura, S., Shioda, T. & Nagai, Y. (2001).** Quintuple deglycosylation mutant of simian immunodeficiency virus SIVmac239 in rhesus macaques: robust primary replication, tightly contained chronic infection, and elicitation of potent immunity against the parental wild-type strain. *J Virol* **75**, 4023–4028.

**Mori, K., Sugimoto, C., Ohgimoto, S., Nakayama, E. E., Shioda, T., Kusagawa, S., Takebe, Y., Kano, M., Matano, T. & other authors (2005).** Influence of glycosylation on the efficacy of an Env-based vaccine against simian immunodeficiency virus SIVmac239 in a macaque AIDS model. *J Virol* **79**, 10386–10396.

**Muster, T., Steindl, F., Purtscher, M., Trkola, A., Klima, A., Himmler, G., Ruker, F. & Katinger, H. (1993).** A conserved neutralizing epitope on gp41 of human immunodeficiency virus type 1. *J Virol* **67**, 6642–6647.

**Nishimura, Y., Igarashi, T., Haigwood, N., Sadjadpour, R., Plishka, R. J., Buckler-White, A., Shibata, R. & Martin, M. A. (2002).** Determination of a statistically valid neutralization titer in plasma that confers protection against simian-human immunodeficiency virus challenge following passive transfer of high-titered neutralizing antibodies. *J Virol* **76**, 2123–2130.

**Nyambi, P. N., Gorny, M. K., Bastiani, L., van der Groen, G., Williams, C. & Zolla-Pazner, S. (1998).** Mapping of epitopes exposed on intact human immunodeficiency virus type 1 (HIV-1) virions: a new strategy for studying the immunologic relatedness of HIV-1. *J Virol* **72**, 9384–9391.

**O'Connor, D. H., Mothe, B. R., Weinfurter, J. T., Fuenger, S., Rehrauer, W. M., Jing, P., Rudersdorf, R. R., Liebl, M. E., Krebs, K. & other authors (2003).** Major histocompatibility complex class I alleles associated with slow simian immunodeficiency virus disease progression bind epitopes recognized by dominant acute-phase cytotoxic-T-lymphocyte responses. *J Virol* **77**, 9029–9040.

**Ohgimoto, S., Shioda, T., Mori, K., Nakayama, E. E., Hu, H. & Nagai, Y. (1998).** Location-specific, unequal contribution of the *N* glycans in simian immunodeficiency virus gp120 to viral infectivity and removal of multiple glycans without disturbing infectivity. *J Virol* **72**, 8365–8370.

**Pinschewer, D. D., Perez, M., Jeetendra, E., Bachi, T., Horvath, E., Hengartner, H., Whitt, M. A., de la Torre, J. C. & Zinkernagel, R. M. (2004).** Kinetics of protective antibodies are determined by the viral surface antigen. *J Clin Invest* **114**, 988–993.

**Puffer, B. A., Pohlmann, S., Edinger, A. L., Carlin, D., Sanchez, M. D., Reitter, J., Watry, D. D., Fox, H. S., Desrosiers, R. C. & Doms, R. W. (2002).** CD4 independence of simian immunodeficiency virus Envs is associated with macrophage tropism, neutralization sensitivity, and attenuated pathogenicity. *J Virol* **76**, 2595–2605.

**Regier, D. A. & Desrosiers, R. C. (1990).** The complete nucleotide sequence of a pathogenic molecular clone of simian immunodeficiency virus. *AIDS Res Hum Retroviruses* **6**, 1221–1231.

**Reimann, K. A., Parker, R. A., Seaman, M. S., Beaudry, K., Beddall, M., Peterson, L., Williams, K. C., Veazey, R. S., Montefiori, D. C. & other authors (2005).** Pathogenicity of simian-human immunodeficiency virus SHIV-89.6P and SIVmac is attenuated in cynomolgus macaques and associated with early T-lymphocyte responses. *J Virol* **79**, 8878–8885.

**Reitter, J. N., Means, R. E. & Desrosiers, R. C. (1998).** A role for carbohydrates in immune evasion in AIDS. *Nat Med* **4**, 679–684.

**Schmitz, J. E., Johnson, R. P., McClure, H. M., Manson, K. H., Wyand, M. S., Kuroda, M. J., Lifton, M. A., Khunkhun, R. S., McEvers, K. J. & other authors (2005).** Effect of $CD8^+$ lymphocyte depletion on virus containment after simian immunodeficiency virus SIVmac251 challenge of live attenuated SIVmac239Δ3-vaccinated rhesus macaques. *J Virol* **79**, 8131–8141.

**Silvera, P., Flanagan, B., Kent, K., Rud, E., Powell, C., Corcoran, T., Bruck, C., Thiriart, C., Haigwood, N. L. & Stott, E. J. (1994).** Fine analysis of humoral antibody response to envelope glycoprotein of SIV in infected and vaccinated macaques. *AIDS Res Hum Retroviruses* **10**, 1295–1304.

**Smith, D. G. & McDonough, J. (2005).** Mitochondrial DNA variation in Chinese and Indian rhesus macaques (*Macaca mulatta*). *Am J Primatol* **65**, 1–25.

**Wei, X., Decker, J. M., Wang, S., Hui, H., Kappes, J. C., Wu, X., Salazar-Gonzalez, J. F., Salazar, M. G., Kilby, J. M. & other authors (2003).** Antibody neutralization and escape by HIV-1. *Nature* **422**, 307–312.

**Wyatt, R. & Sodroski, J. (1998).** The HIV-1 envelope glycoproteins: fusogens, antigens, and immunogens. *Science* **280**, 1884–1888.

**Wyatt, R., Kwong, P. D., Desjardins, E., Sweet, R. W., Robinson, J., Hendrickson, W. A. & Sodroski, J. G. (1998).** The antigenic structure of the HIV gp120 envelope glycoprotein. *Nature* **393**, 705–711.

**York, J. & Nunberg, J. H. (2004).** Role of hydrophobic residues in the central ectodomain of gp41 in maintaining the association between human immunodeficiency virus type 1 envelope glycoprotein subunits gp120 and gp41. *J Virol* **78**, 4921–4926.